SANDIA REPORT

SAND2010-7314
Unlimited Release
Printed October 2010

Statistical Criteria for Characterizing Irradiance Time Series

Clifford W. Hansen, Joshua S. Stein, and Abraham Ellis

Prepared by
Sandia National Laboratories
Albuquerque, New Mexico 87185 and Livermore, California 94550

Sandia National Laboratories is a multi-program laboratory managed and operated by Sandia Corporation, a wholly owned subsidiary of Lockheed Martin Corporation, for the U.S. Department of Energy's National Nuclear Security Administration under contract DE-AC04-94AL85000.

Issued by Sandia National Laboratories, operated for the United States Department of Energy by Sandia Corporation.

Available to DOE and DOE contractors from
U.S. Department of Energy
Office of Scientific and Technical Information
P.O. Box 62
Oak Ridge, TN 37831

Telephone: (865) 576-8401
Facsimile: (865) 576-5728
E-Mail: reports@adonis.osti.gov
Online ordering: http://www.osti.gov/bridge

Available to the public from
U.S. Department of Commerce
National Technical Information Service
5285 Port Royal Rd.
Springfield, VA 22161

Telephone: (800) 553-6847
Facsimile: (703) 605-6900
E-Mail: orders@ntis.fedworld.gov
Online order: http://www.ntis.gov/help/ordermethods.asp?loc=7-4-0#online

SAND2010-7314
Unlimited Release
Printed October 2010

Statistical Criteria for Characterizing Irradiance Time Series

Clifford W. Hansen, Joshua S. Stein, and Abraham Ellis
Photovoltaics and Grid Integration
Sandia National Laboratories
P.O. Box 5800
Albuquerque, New Mexico 87185-MS1033

Abstract

We propose and examine several statistical criteria for characterizing time series of solar irradiance. Time series of irradiance are used in analyses that seek to quantify the performance of photovoltaic (PV) power systems over time. Time series of irradiance are either measured or are simulated using models. Simulations of irradiance are often calibrated to or generated from statistics for observed irradiance and simulations are validated by comparing the simulation output to the observed irradiance. Criteria used in this comparison should derive from the context of the analyses in which the simulated irradiance is to be used. We examine three statistics that characterize time series and their use as criteria for comparing time series. We demonstrate these statistics using observed irradiance data recorded in August 2007 in Las Vegas, Nevada, and in June 2009 in Albuquerque, New Mexico.

ACKNOWLEDGMENTS

We wish to acknowledge the Las Vegas Valley Water District and SunPower Corporation for granting access to the irradiance dataset from Las Vegas, Nevada.

CONTENTS

FIGURES

TABLES

NOMENCLATURE

CSP	concentrated solar power
DOE	Department of Energy
PV	photovoltaic
SNL	Sandia National Laboratories

1. INTRODUCTION

The amount of solar generation on the electrical grid is projected to increase rapidly and will reach high penetration levels in parts of the system. Due to the variable nature of its output, solar generation (especially photovoltaic (PV) and concentrated solar power (CSP) without energy storage) has the potential to affect power system operations in several ways. Variable flow on distribution and transmission lines could degrade power quality by introducing voltage variations and thus impose stress on voltage control equipment. At the system level, variability complicates efforts by utilities to meet power balancing requirements or to minimize the cost of energy production. Industry experience is insufficient to allay concerns about the potential impact of high solar penetration, and the pace of solar generation deployment is hindered by the perceived risk of unacceptable system variability. Thus, methods for assessing the impact of solar generation on grid operations are currently of great interest.

It is possible to estimate the impact of variable generation on the grid. Over the last decade, methodologies for studying the effects of wind generation have been refined and validated to some extent (e.g., [1]). Fundamentally, the effects are functions of the grid characteristics (local network and balancing area), the flexibility of automatic generation control systems and other market mechanisms available to grid operators, the temporal variability of the variable resource being considered (i.e., seasonal, daily, hourly and sub-hourly patterns), and the spatial separation of generators. Integration studies at the regional scale require estimates of the output from variable generation sources that is weather-consistent and time-synchronized with the load. For integration studies involving wind generation, mesoscale numerical weather models are used to produce hourly and 10-minute wind and power output estimates. However, similar techniques to estimate solar irradiance and output from solar generation do not currently exist.

Generally speaking, the variability of solar generation is driven by the variability of the solar resource (irradiance). Therefore, a model that produces estimates of irradiance at short time scales is a key first step in estimating solar plant output. Irradiance models should produce estimates that are statistically consistent with observations of irradiance, which are available for many locations in the US, with records that span several decades albeit with relatively coarse spatial and (with some exceptions) temporal resolution. Determining statistical consistency requires selection of statistics to be used to compare simulations with observations. This report first proposes a relatively small set of statistics for characterizing time series of irradiance, and examines the use of these statistics as criteria for comparing model output to observations in order to judge statistical consistency.

1.1. Notation and Assumptions

Measurements of solar irradiance on a horizontal plane can be represented mathematically as a time series $\{R(t,\mathbf{x})\}$ where t is time and $\mathbf{x}$ is a vector indicating location in a coordinate system. Formally $\{R(t,\mathbf{x})\}$ can be regarded as a stochastic process indexed by time t with state space comprising random fields of irradiance values at each point $\mathbf{x}$. However, $\{R(t,\mathbf{x})\}$ is not stationary due to the diurnal and annual variation in solar irradiance due to the sun's changing

zenith angle. To remove these effects and obtain a stochastic process that may be regarded as stationary, irradiance is often normalized by dividing irradiance at the earth's surface by the irradiance expected for clear sky conditions; which can be simulated from commonly available weather data. The resulting quotient is termed the *clearness index* and is denoted here as $\{C(t,\mathbf{x})\}$. Converting to clearness index permits comparison of irradiance measurements at different times and on different calendar days but with loss of information about the magnitude of irradiance.

In this paper, we consider irradiance and clearness index only at a single point and simplify our notation by omitting $\mathbf{x}$. The determination of spatial correlations in irradiance or clearness index is an important problem which we do not take up in this paper. Usually observed or simulated values are obtained at a discrete sequence of times $\{t_j\}$. Thus, for example, a collection of independent realizations of the stochastic process for clearness index at the point $\mathbf{x}$ are indicated by $C_i(t_j)$ where *i* indexes the realizations.

We assume that the transformation from irradiance to clearness index is effective at removing diurnal variations and results in a weakly stationary stochastic process, that is, the mean and variance for time series of clearness index do not depend on the time of day. This assumption is clearly not appropriate for irradiance as irradiance is subject to diurnal cycles. Irradiance may vary on longer cycles, such as non-stationary weather cycles (e.g. warm or cold air masses which bring different cloud conditions) and annual variation in global solar irradiance. Where such influences are present in observed irradiance and the assumption of stationarity is made, analysts should take care to subdivide the time series into periods for which the stationarity assumption is appropriate (e.g., periods with similar cloud conditions, calendar periods, etc.).

2. METRICS FOR CHARACTERIZING TIME SERIES

Time series of irradiance or clearness index are often generated to support economic or operational analyses of solar power systems. For example, an analysis may be conducted to determine the expected return on investment from a proposed solar power plant. In this kind of analysis, the analysis inputs representing the solar resource should be consistent with the levels of solar irradiance at the site under consideration; otherwise, the analysis risks under- or over-estimating the economic gain. Other analyses may examine strategies for mitigating the variability in power output resulting from temporal variability in the solar resource; such analyses require inputs that are consistent with both the level of irradiance and changes in level of the solar resource. The suitability of a model for simulating irradiance should thus be judged in the context of the analysis that the model will support.

Fundamentally, simulated irradiance should be statistically consistent with observed or measured irradiance. One method of constructing synthetic time series of irradiance that are statistically consistent with a set of observations is to select representative periods from the observations and to concatenate the selected periods to form time series. The resulting time series are often referred to as 'representative' months or years (e.g., [2, 3].) This method has the advantages of simplicity and of maintaining consistency with the observations, but also has drawbacks. The representative time series is constrained to replaying historical data, which may not be representative of the full range of variability that could occur. Consequently, we prefer criteria phrased in terms of statistics estimated from recorded data. Simulations of irradiance (using models and appropriate sampling methods) are then compared to observations using these statistics.

Determining statistical consistency first requires identification of the statistics to be considered. Our selection of statistics is guided by the aspects of the solar resource that are likely to be significant in analyses of solar power systems, namely, the level of irradiance and the changes in irradiance over time. We prefer to compare model output with observations using only a few statistics to avoid over-constraining model output. We propose here three statistics that can be used to compare simulations to observed data to judge consistency:

1. The frequency distribution of irradiance (or clearness index). The frequency distribution quantifies the fraction of time that irradiance falls within a specified range of values.

2. The distribution of ramps (i.e., changes in level) of irradiance (or clearness index) over a period of time.

3. The autocovariance and autocorrelations in the time series of clearness index and of ramps in clearness index.

The frequency distribution of irradiance, $F(R)$, quantifies the fractional time (within the time period of interest) that irradiance is less than a specified value, i.e., $F(R) = P(R \le r)$; here $F(R)$ denotes the cumulative distribution. The probability density function $f(R)$

corresponding to the distribution $F(R)$ can be approximated by a histogram produced from the data $\bigcup_{i,j} C_i(t_j)$, where the union is taken over the data on which the simulations will be based. The frequency distribution of irradiance is important for analyses that estimate the value of the solar resource over a period of time. Because power output changes rapidly with changes in the level of irradiance, for all but very short time intervals, power at time t_j is independent of power at other times. Thus, the distribution of power is reasonably given by $Power(P) = F(T(R))$ where $T(R)$ is a function that translates irradiance to power. Typically, this function may consider module and inverter technology, temperature, the angle of incidence and spectral characteristics of the light hitting the PV array as inputs (e.g., [4]).

Other methods for characterizing irradiance variability have been proposed. Models based on Fourier transforms have been used to represent sequences of daily overall global solar irradiation (e.g., Sun and Kok, 2007 [5]; Baldasano et al., 1988 [6]), but have not proven to be suitable for representing variability at shorter time intervals (e.g., hours or minutes) because short-term (intraday) variations are not periodic. Woyte et al. (2007a; 2007b [7, 8]) have suggested characterizing irradiance by a localized spectral analysis using a wavelet decomposition. Their approach aims to characterize the amplitude, persistence, and frequency of occurrence of fluctuations without focusing on when the fluctuations occur in time. They do not suggest an algorithm for simulating irradiance time series, but their approach may prove useful for comparing measured and simulated irradiance. We plan to evaluate this approach in future work, but do not consider it further in this report.

Typically irradiance is measured as an average over a measurement time interval and thus observed irradiance and clearness index are both time-averaged quantities. Analyses of clearness index (many of which are summarized in Tovar-Pescador, 2008 [9]) have considered time intervals for this averaging ranging from 24hr (i.e., daily clearness index) to as short at 30s (Glasbey, 2001 [10]); one second observations are also available (Kuszamaul et al. 2010 [11]]). The time interval for averaging should be carefully chosen to match the desired goals of the analysis, because the interval is quite influential on the frequency distribution for clearness index (e.g., Gansler et al., 1995 [12]). Speaking generally, frequency distributions of daily clearness index tend to be asymmetric with a peak around a value of one and a long tail towards values of zero. When the measurement time interval is sufficiently short (e.g., 1 min) the frequency distribution of clearness index tends to be distinctly bimodal with peaks at one and at a value less than one resulting from the occlusion of the irradiance sensor by clouds; examples are given in (Gansler et al., 1995 [12]; Tovar et al., 1998;1999; 2001 [13, 14, 15]).

The second statistic, the distribution of ramps, informs analyses that examine the effects of variability in the solar resource on the power grid and the value of strategies to manage the variability. Grid management entails mitigating any rapid changes in power output that can result from rapid changes in irradiance. Evaluating the effectiveness of management strategies requires representing the effects on power output of changes in irradiance with sufficient fidelity. The distribution of ramps serves this purpose by quantifying the probability of observing ramps of varying duration and magnitude during the period of interest.

Conceptually, change in irradiance can be quantified by the derivative $\frac{dR(t)}{dt}$ with the derivative approximated by the ratio $\frac{dR(t)}{dt} \cong \frac{R(t_{j+1}) - R(t_j)}{t_{J+1} - t_j}$ because irradiance is not observed continuously. However, using a constant time interval $\Delta t = t_{J+1} - t_j$ in this approximation is problematic; if the time interval is small, the resulting sequence of slopes will represent large magnitude, long duration changes as a sequence of short, small changes, whereas the approximation may omit short duration changes if the time interval is too large. Consequently, we propose that changes in irradiance first be approximated by a sequence of line segments by fitting the data with a piecewise linear function designed to overcome the limitation of fixed time intervals.

Generally, a fitting algorithm analyzes a time series of clearness index and identifies dominant points which, when connected, approximate the time series with a set of line segments (using the dominant points as vertices). Each line segment represents a ramp event, characterized by duration and magnitude (see Figure 1). For a sequence of irradiance $R_i(t)$, the algorithm produces a sequence of ordered pairs $\left\{\left(\Delta R_j, \Delta t_j\right)_i\right\}$ where ΔR_j is the change in irradiance level of duration Δt_j. Once the sequences $\left\{\left(\Delta R_j, \Delta t_j\right)_i\right\}$ are obtained, the ramps in irradiance are regarded as jointly distributed random variables, and the joint distribution of (R,t) is approximated by the bivariate histogram obtained from $\bigcup_{i,j}\left(\Delta R_j, \Delta T_j\right)_i$.

There exist several methods for identifying dominant points. One relatively simple and robust approach is the 'swinging door' algorithm (Bristol, 1990 [16]). This algorithm has been used to quantify ramps in load and power in analyses of the operational impacts on the electrical grid of wind generation (Makarov et al 2009 [17]). The algorithm chooses dominant points such that each data falls within a given vertical tolerance limit of the line segment joining its adjacent dominant points. The swinging door method has the advantage that the tolerance limit is specified in units of irradiance or as a fraction of clear-sky irradiance (i.e., clearness index value). Another similar algorithm is the 'arc-chord' method (Horst and Beichel, 1996 [18]). This method assigns the first point as a dominant point and looks at future values and calculates the length of the arc (sum of line segments connecting adjacent points) and the length of the chord (straight line distance between dominant point and point being examined). Once the difference between arc and chord length exceeds a tolerance limit, the previous point becomes a new dominant point and the process proceeds. A further step loops through all dominant points and removes points that fall within a certain distance from the line connecting surrounding dominant points. The arch-chord method has the disadvantage that the tolerance limit is a distance in the time-irradiance coordinate system and thus does not have intuitive units.

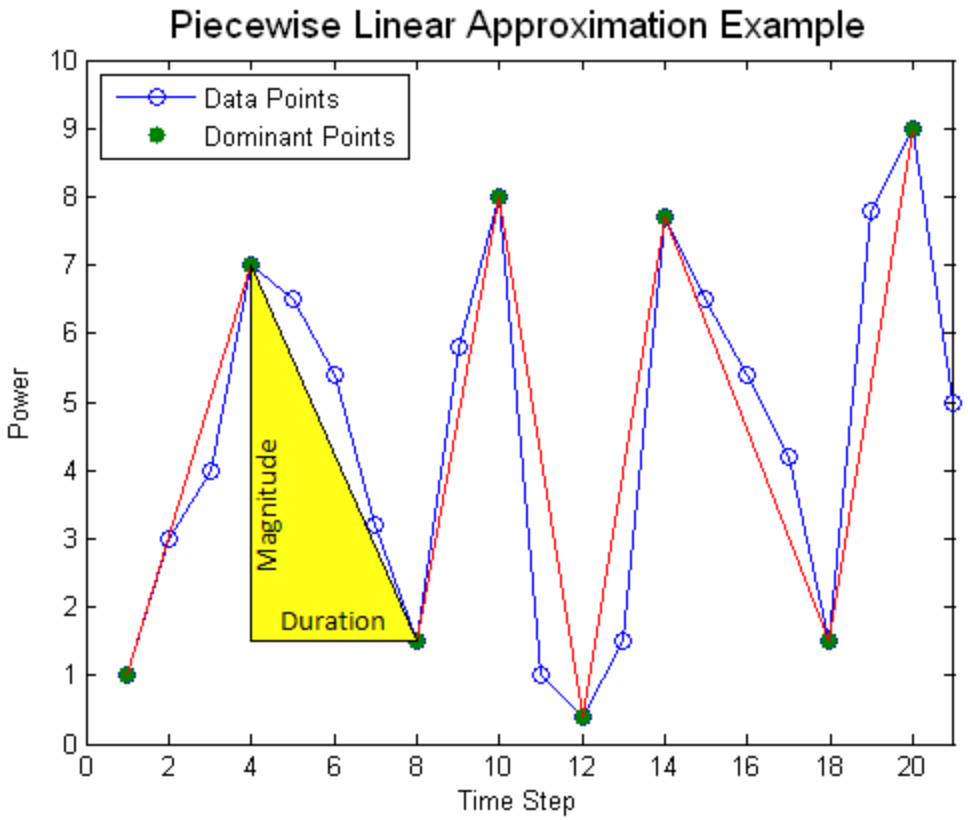

Figure 1. Example of Piecewise Linear Approximation.

By themselves, the frequency distribution of irradiance (first statistic) and the bivariate distribution of ramps (second statistic) are not sufficient to describe the stochastic process underlying the time series of irradiance, because these distributions do not capture correlations between values in the time series. If an analysis depends on the sequence of irradiance values or ramps (rather than just the frequencies of levels of irradiance or of ramps), irradiance simulations should appropriately account for correlations between values. These correlations may be characterized by the autocovariance and the autocorrelation coefficient. These statistics are not informative when the underlying time series are not stationary. Consequently we examine the autocovariance and the autocorrelation coefficient only for clearness index and for ramps in clearness index.

Given a time series $C(t_j)$, $j=1,\ldots,n$ with mean $\bar{C}=\frac{1}{n}\sum_{i=1}^{n}C(t_j)$ the autocovariance at lag k, denoted by $K(k)$, is estimated by $K(k)=\sum_{i=1}^{N-k}\left(C(t_i)-\bar{C}\right)\left(C(t_{i+k})-\bar{C}\right)$ and the autocorrelation coefficient, denoted by $r(k)$, is estimated by $r(k)=\dfrac{\sum_{i=1}^{N-k}\left(C(t_i)-\bar{C}\right)\left(C(t_{i+k})-\bar{C}\right)}{\sum_{i=1}^{N}\left(C(t_i)-\bar{C}\right)^2}$ (assuming that the time series is weakly stationary). The autocovariance coefficient is positive at lag *k* when the

time series that results by shifting C by k units is similar to C itself (i.e. is correlated with C). The autocorrelation coefficient is the autocovariance normalized by the variance of the time series and thus is scale independent.

For the bivariate time series of ramps, two autocovariances (and autocorrelation coefficients) and one cross-covariance (and cross-correlation coefficient) are obtained, each of the form $K_{X,Y}(k) = \sum_{i=1}^{N-k} \left(X(t_i) - \bar{X} \right) \left(Y(t_{i+k}) - \bar{Y} \right)$ or $r_{X,Y}(k) = \frac{\sum_{i=1}^{N-k} \left(X(t_i) - \bar{X} \right) \left(Y(t_{i+k}) - \bar{Y} \right)}{\sqrt{\sum_{i=1}^{N} \left(X(t_i) - \bar{X} \right)^2} \sqrt{\sum_{i=1}^{N} \left(Y(t_i) - \bar{Y} \right)^2}}$ where X and Y are chosen from R or T. The correlation coefficients quantify the degree of statistical dependence between values at different times in the time series. We note that autocovariances and autocorrelation coefficients do not completely characterize correlations in the time series, in the same sense that means and standard deviations do not completely characterize probability distributions.

The frequency distribution of clearness index has been the subject of extensive evaluation. Numerous models for this distribution have been published, as summarized by Tovar [9]. Most analyses examine relatively long (daily or hourly) intervals for clearness index; a few analyses (e.g., Glasbey (2001), [10]) examined clearness index for short (30s or 1 minute) intervals. Few analyses of the distribution of ramps in clearness index are published. Makarov et al [17] considered distributions of power ramps in an analysis of the operational impact of wind power generation. Tomson et al. (2008) describe the distribution of ramp magnitudes for five-minute averages of irradiance [19]. Autocorrelation in clearness index was recognized by many as an important process to represent in models of irradiance (e.g., Skartveit and Olseth (1992) [20]; Walkenhorst et al. (2002) [21]). They developed irradiance simulation algorithms which aimed to match observed frequency distributions and autocorrelation characteristics of clearness index time series. However, their model forms have not been tested to determine how well simulations match distributions of ramps.

3. APPLICATION OF CRITERIA TO IRRADIANCE DATA

We illustrate these criteria using irradiance data collected in Las Vegas, Nevada in August 2007 and in Albuquerque, New Mexico, in June 2009.

3.1 Irradiance Data for Las Vegas

One-minute averages of irradiance were recorded by the Las Vegas Valley Water District at a ~400 kW photovoltaic array at Las Vegas Springs Preserve (lat. 36.17N long. 115.19W). Irradiance measurements are converted to clearness index using the Atwater and Ball (1979 [22]) model for clear sky global irradiance. This model requires as input total precipitable water, air pressure, ground and sky albedo, and broadband aerosol optical depth. The model is most sensitive to the value of precipitable water and as a simplifying assumption, we estimated this parameter by fixing the other inputs at reasonable values, which are listed in Table 1, and minimizing the sum of the least-squared error for selected clear days in August 2007. Model prediction of clear sky irradiance at the beginning and end of the day are the most uncertain and therefore only irradiance values between 9am PDT and 4pm PDT are considered here.

Table 1. Parameters used for Clear Sky Irradiance Model

Parameter	**Value**	**Units**	**Source**
Precipitable water	2.6	cm	Fitted
Air Pressure	950	mbar	estimate
Ground Albedo	0.2	[]	estimate
Sky Albedo	0.0685	[]	Bird and Hulstrom, 1981 [23]
Aerosol Optical Depth	0.05	[]	Flowers et al., 1969 [24]

Figure 2 shows irradiance for the selected time period; Figure 3 illustrates clearness index. Clear sky conditions are evident for about half of the days as indicated by smoothly varying irradiance and clearness index nearly constant at a value of approximately one. Cloudy conditions are also present resulting in large changes in irradiance (e.g., 2007/08/02) or in generally overcast conditions (e.g. 2007/08/01). Clearness index may exceed one for brief intervals of time due to *cloud enhancement*, where cloud edges near the position of the sun reflect additional light to the ground and briefly causing irradiance to exceed that measured on a clear day [25, 26].

Figure 4 and Figure 5 illustrate the frequency distributions of irradiance and clearness index, respectively, for the Las Vegas Springs Preserve irradiance data, using histograms of the observed values. The corresponding probability density functions may be estimated from the histograms by dividing by the total number of observations. An optimal bin size for each histogram (27 $W/m^2$and 0.029 for irradiance and clearness index, respectively) was determined using the criteria outlined by Shimazaki and Shinomoto (2007 [27]). The distributions are similar in shape, with a large peak resulting from predominantly clear sky conditions. The irradiance peak is more broad than the clearness index peak, because irradiance levels vary

throughout the time period considered (i.e., between 9am and 4pm) but clearness index does not vary during clear sky conditions.

Figure 6 illustrates the use of the piecewise linear approximation to irradiance for two days, August 2, 2007 and August 5, 2007, during which cloudy and clear sky conditions respectively, are observed. This approximation was made using the swinging door algorithm with a tolerance of 20 W/m^2, i.e., each observed irradiance value is within 20 W/m^2 of the concurrent approximation value. The figure shows that the approximation reasonably follows the changes in the irradiance level.

Figure 7 illustrates the bivariate distribution of ramps in irradiance calculated from the piecewise linear approximations for August 2007, two days from which are illustrated in Figure 5. The shape of this histogram depends in part on the tolerance set for the piecewise linear approximation (here, 20 W/m^2) as well as on the number of bins chosen for each axis (50 in this case). Most ramps in irradiance are short and of relatively small magnitude; 65% of the ramps in Figure 7 have duration 2 minutes or less, and of these ramps, 85% (55% of all ramps) are of magnitude 100 W/m^2 or less. The symmetrical appearance of the distribution of these ramps results because irradiance first increases then decreases during the time period considered. A relatively small number of ramps are of low magnitude but longer duration as indicated by the ridge extended along magnitude between -17 and 13 (i.e., the bins centered roughly on duration of zero).

Figure 8a illustrates the bivariate distribution of ramps in clearness index calculated from the piecewise linear approximations for August 2007, computed with tolerance 0.02 and using 50 bins for each axis. The histogram for clearness index appears similar to the histogram for irradiance, although the piecewise linear approximation to the clearness index curves allows for ramps of much longer duration. Figure 8b presents a scatterplot of ramp duration and magnitude and clearly shows the predominance of short ramps and the absence of long duration, large magnitude ramps. The relatively small number of ramps of long duration is a direct consequence of approximating clearness index with a piecewise linear function. This approximation method represents clearness index for a clear day with relatively few (i.e., two or three) line segments, whereas clearness index for a cloudy day is represented by many (i.e., 30 or 40) shorter line segments.

The analyses shown in Figure 6 through Figure 8 were repeated using the arc-chord method for piecewise linear approximation rather than the swinging door method. Results similar to those shown in Figure 6 through Figure 8 were obtained.

Figure 9 displays correlograms (i.e., plots of the autocorrelation coefficient and autocovariance as a function of lag) for clearness index for August 2007. One curve is computed for each of the 31 days in August 2007. Curves are shown with blue, dashed lines when the day was entirely clear (as judged by examination of Figure 2); green solid lines are used when the day was partly cloudy. Correlations for irradiance are not shown because such curves are not expected to be informative as the time series of irradiance is not stationary. If correlations were computed for irradiance, the correlation would be primarily determined by the gradual diurnal increase and decrease in irradiance. Generally, autocorrelation coefficients are higher for clear days than for

cloudy days. However, because autocorrelation is normalized by the variance in the clearness index time series, and even for clear days, very small magnitude variations in clearness index are present, autocorrelation curves decay as lag increases for all conditions. Figure 9b shows the autocovariance for clearness index and confirms that no significant variance is present in the time series for clearness index on clear days.

Figure 10 shows correlograms of autocorrelation coefficients for the time series of duration and magnitude of ramps in clearness index. Autocovariance plots (not shown) appear with similar shape but on a different *y*-axis scale. In these correlograms lag is defined in terms of the number of ramps rather than as a difference in time. These statistics were computed by concatenating the sequence of ramps from each day into one sequence of ordered pairs $\{(T,R)\}$. Three plots are shown for each combination of duration (*T*) and ramp magnitude (*R*): *TT*, *RR* and *TR*. The autocorrelation coefficient for ramp duration (Figure 10a) shows that a relatively weak correlation between the duration of successive ramps. Although most ramps are of short duration (Figure 8) the autocorrelation coefficient responds to the small scale variance between ramps of short duration and is not strongly responsive to the relatively rare long duration ramps in this time series.

Figure 10b shows that ramp magnitude is similarly uncorrelated between successive ramps, although the autocorrelation coefficient shows a weak tendency for ramp magnitude to change signs (i.e., an increase in clearness index is somewhat more likely to be followed by a decrease rather than a further subsequent increase). However, after three successive ramps, ramp magnitude is essentially uncorrelated.

Figure 10c shows that the cross-correlation coefficient between ramp duration and magnitude is essentially zero at all lags in the number of ramps. This result is consistent with the scatterplot in Figure 8b which shows an absence of ramps of both long duration and large magnitude.

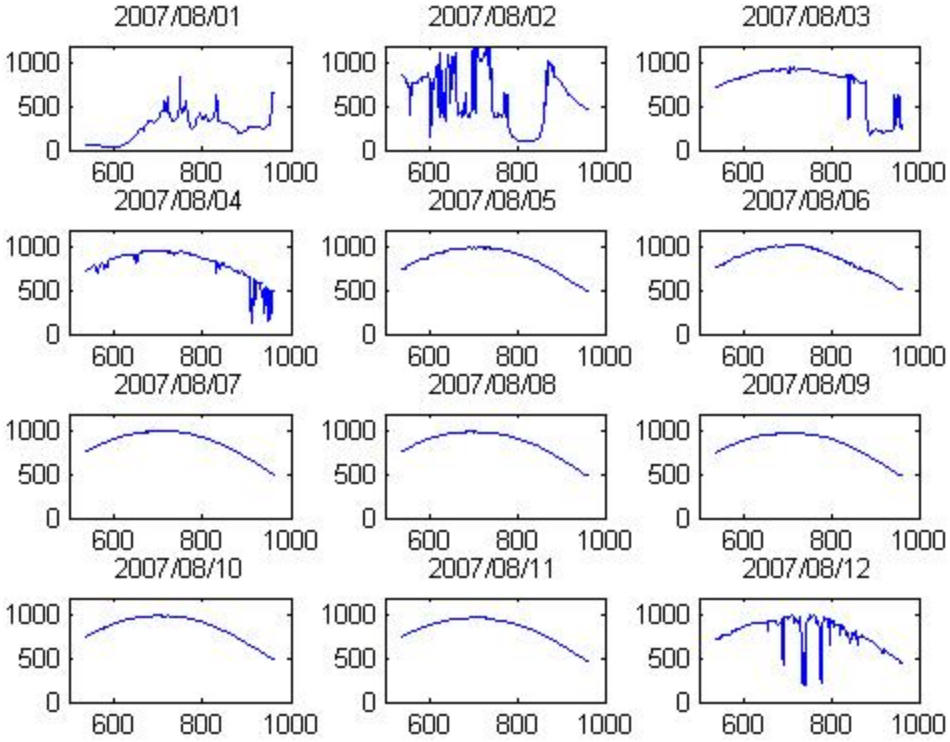
2007/08/01
2007/08/02
2007/08/03
2007/08/04
2007/08/05
2007/08/06
2007/08/07
2007/08/08
2007/08/09
2007/08/10
2007/08/11
2007/08/12
1000
500
0
600
800
1000

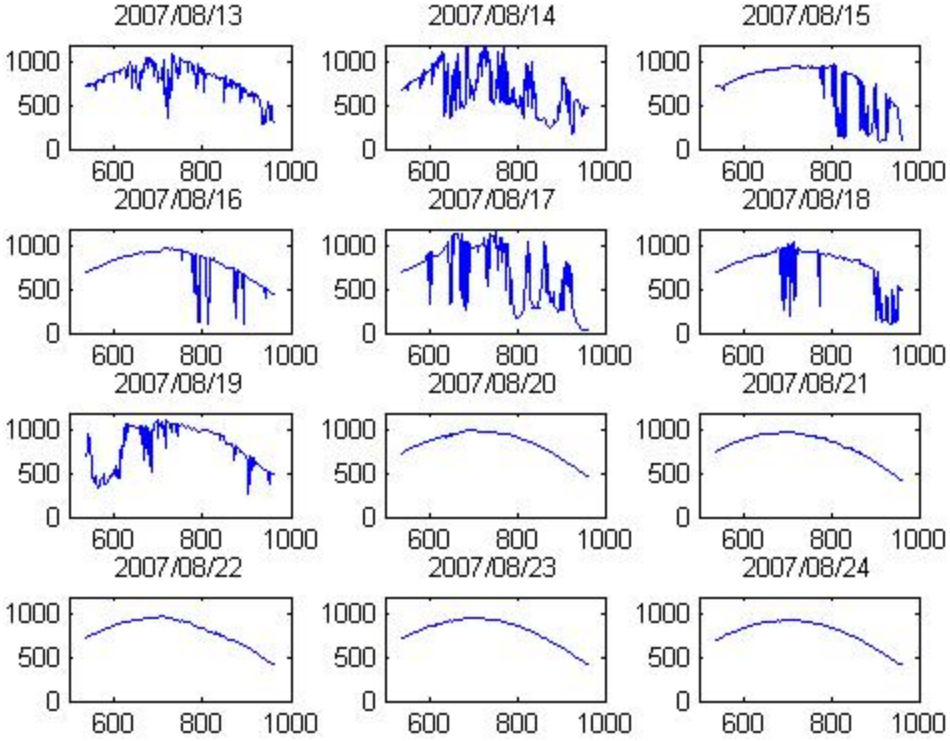
2007/08/13
2007/08/14
2007/08/15
2007/08/16
2007/08/17
2007/08/18
2007/08/19
2007/08/20
2007/08/21
2007/08/22
2007/08/23
2007/08/24
1000
500
0
600
800
1000

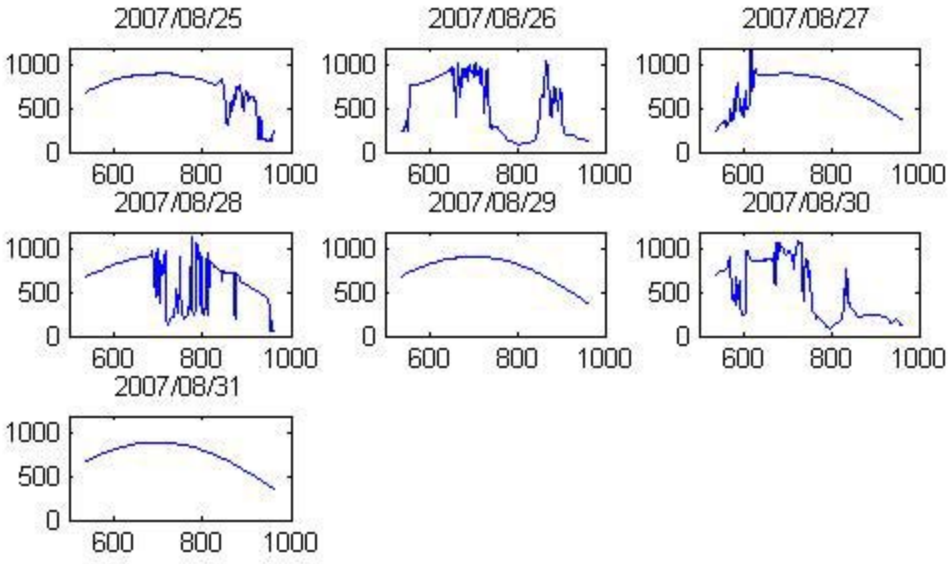

Figure 2. Irradiance recorded during August 2007 at Las Vegas Springs Preserve between 9am PDT and 4pm PDT.

Note: *x*-axis units are minutes since midnight; *y*-axis is irradiance (W/m^2).

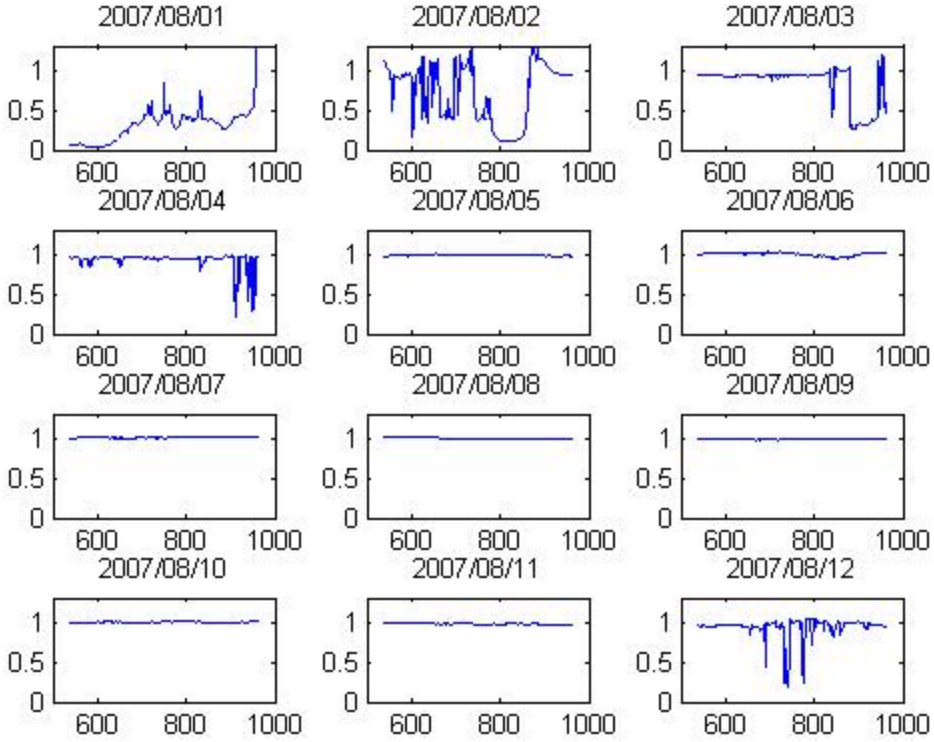
2007/08/01
2007/08/02
2007/08/03
2007/08/04
2007/08/05
2007/08/06
2007/08/07
2007/08/08
2007/08/09
2007/08/10
2007/08/11
2007/08/12
1
0.5
0
600
800
1000

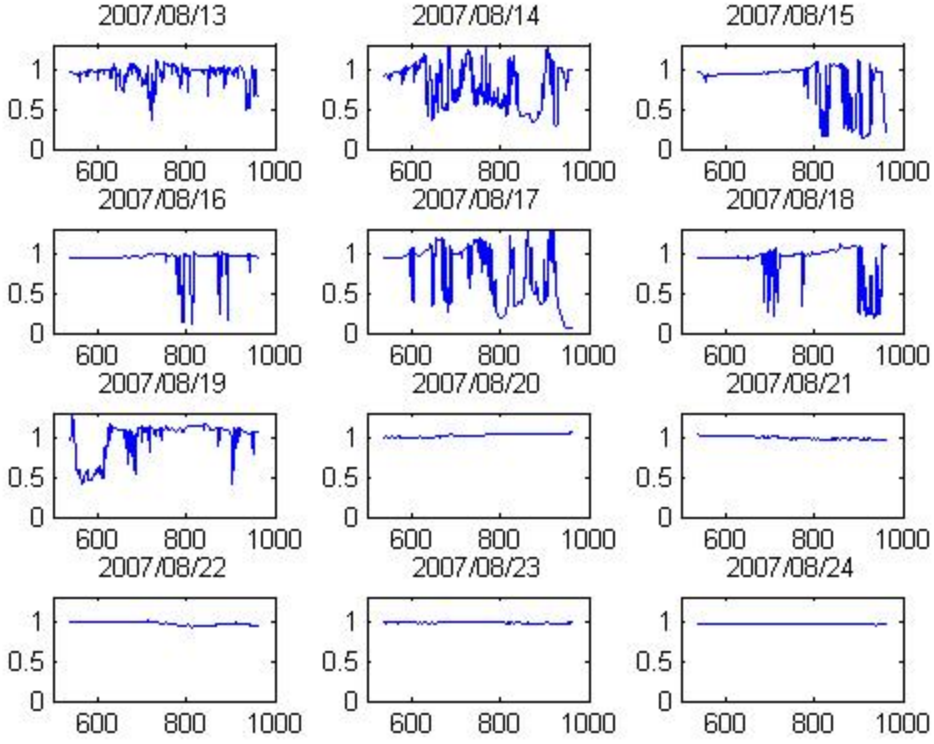
2007/08/13
2007/08/14
2007/08/15
2007/08/16
2007/08/17
2007/08/18
2007/08/19
2007/08/20
2007/08/21
2007/08/22
2007/08/23
2007/08/24
1
0.5
0
600
800
1000

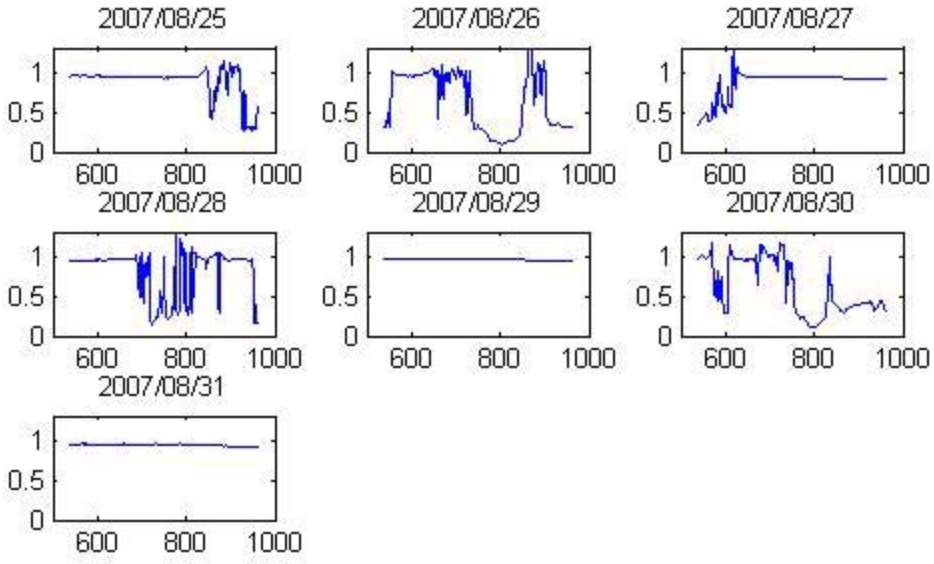

Figure 3. Clearness index for August 2007 at Las Vegas Springs Preserve between 9am PDT and 4 pm PDT.

Note: *x*-axis units are minutes since midnight; *y*-axis is irradiance (W/m^2).

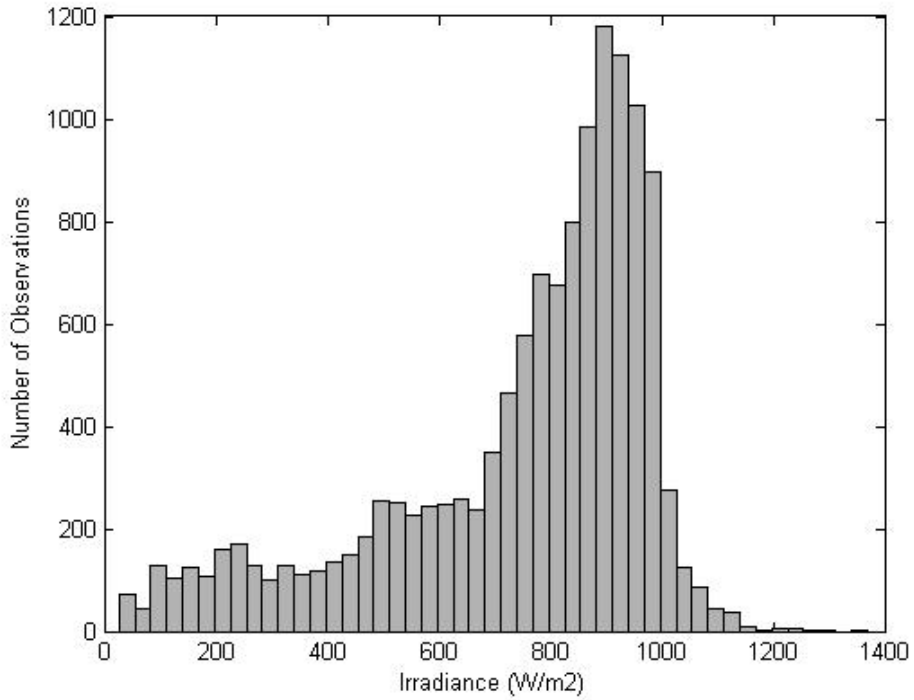

Figure 4. Frequency distribution of irradiance for August 2007, between 9 am PDT and 4 pm PDT, at Las Vegas Springs Preserve.

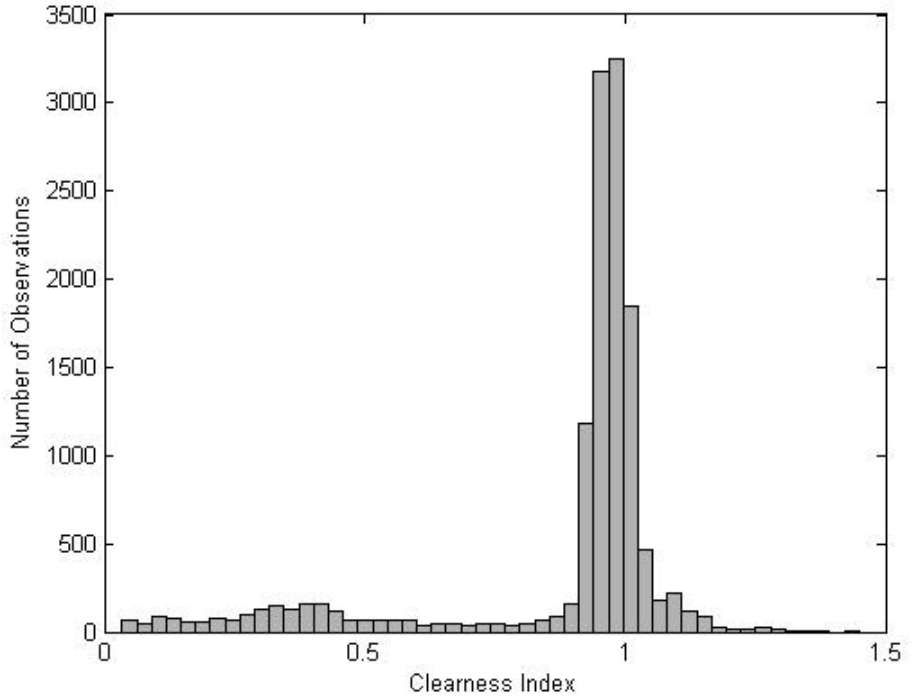

Figure 5. Frequency distribution of clearness index for August 2007, between 9 am PDT and 4 pm PDT, at Las Vegas Springs Preserve.

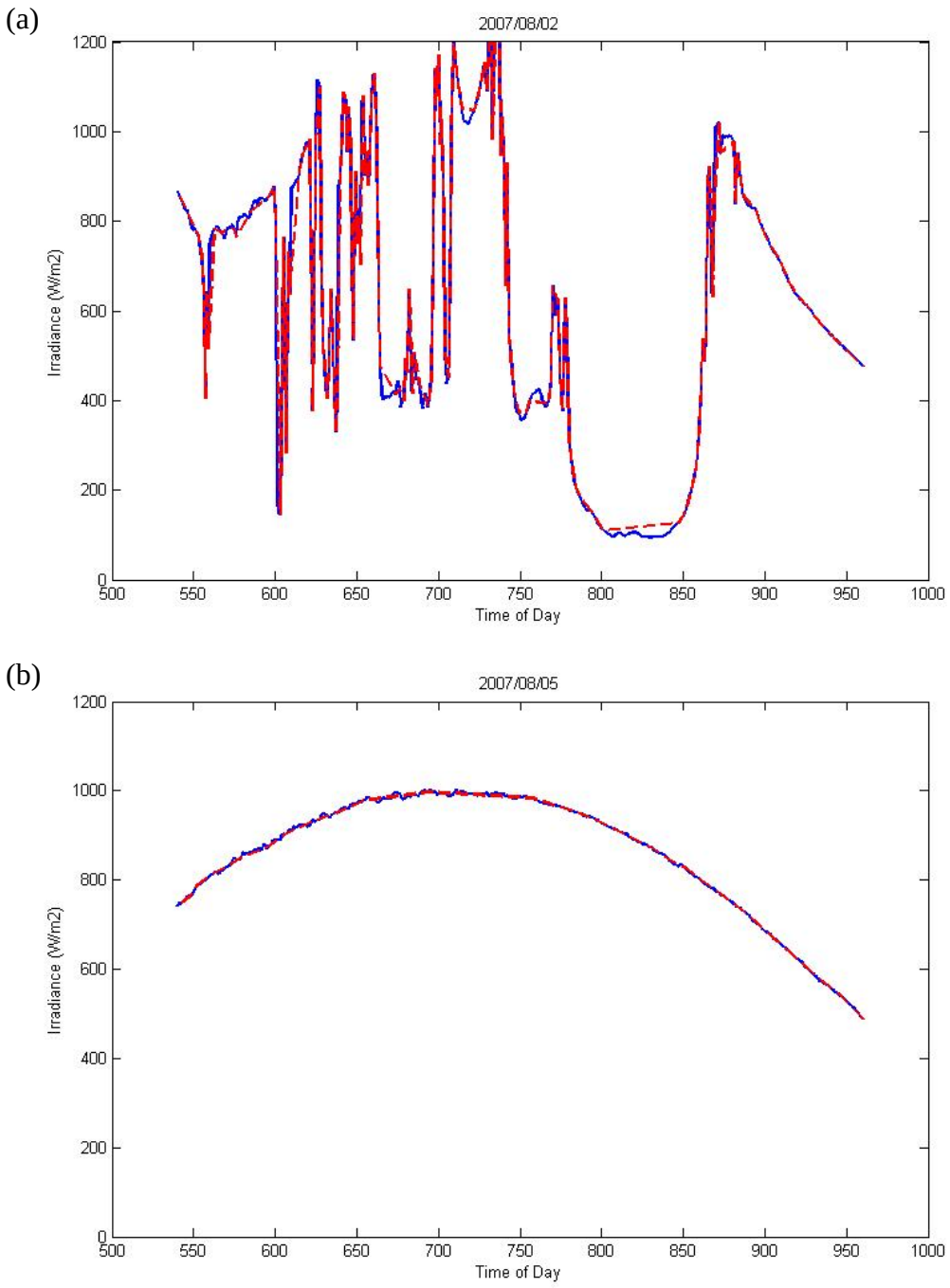

Figure 6. Piecewise linear approximation to irradiance for (a) August 2, 2007 and (b) August 5, 2007 between 9 am PDT and 4 pm PDT, at Las Vegas Springs Preserve.

Note: Irradiance indicated by blue solid line, piecewise linear approximation indicated by red dashed line. Time of day indicated as minutes after midnight.

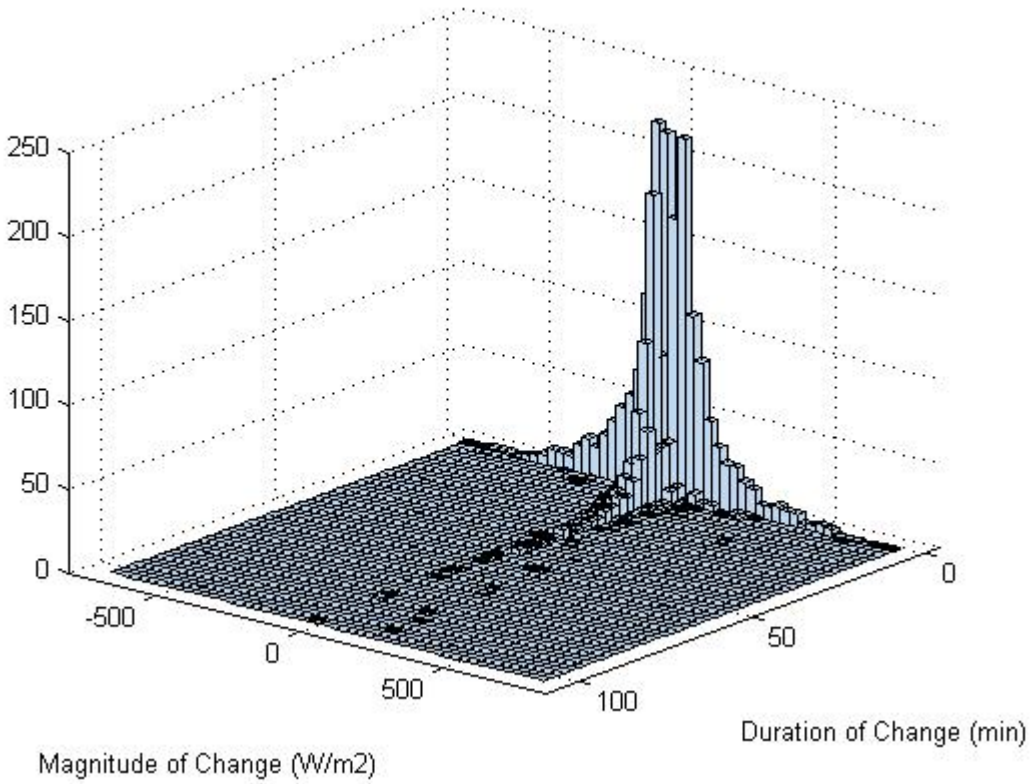

Figure 7. Bivariate histogram of ramps in irradiance calculated using piecewise linear approximation to irradiance for August 2007 between 9 am PDT and 4 pm PDT, at Las Vegas Springs Preserve.

Note: Ramps calculated using piecewise linear approximation to irradiance.

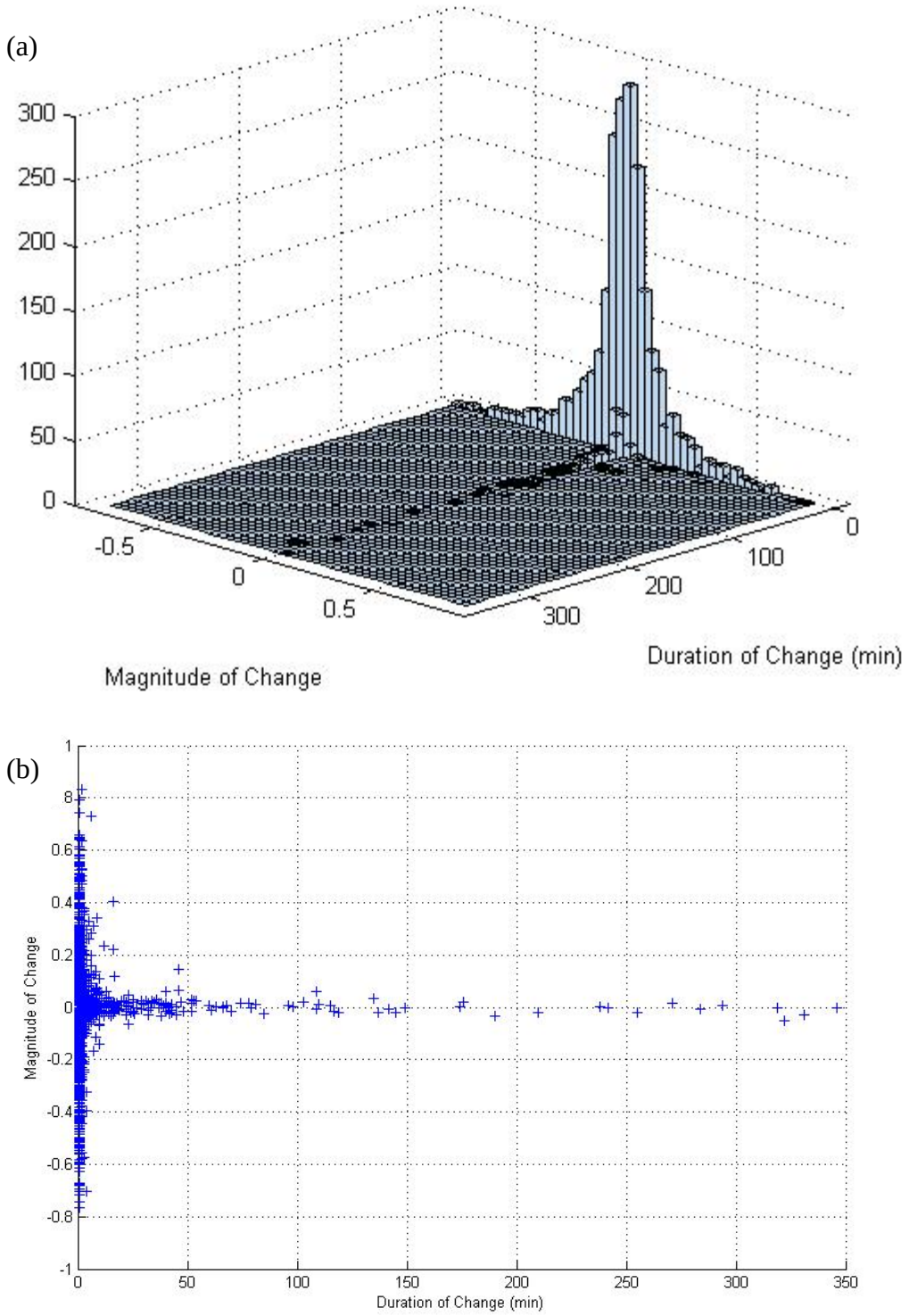

Figure 8. (a) Bivariate histogram of ramps in clearness index and (b) scatterplot of ramp duration and magnitude.

Note: Ramps calculated using piecewise linear approximation to irradiance for August 2007 between 9 am PDT and 4 pm PDT, at Las Vegas Springs Preserve.

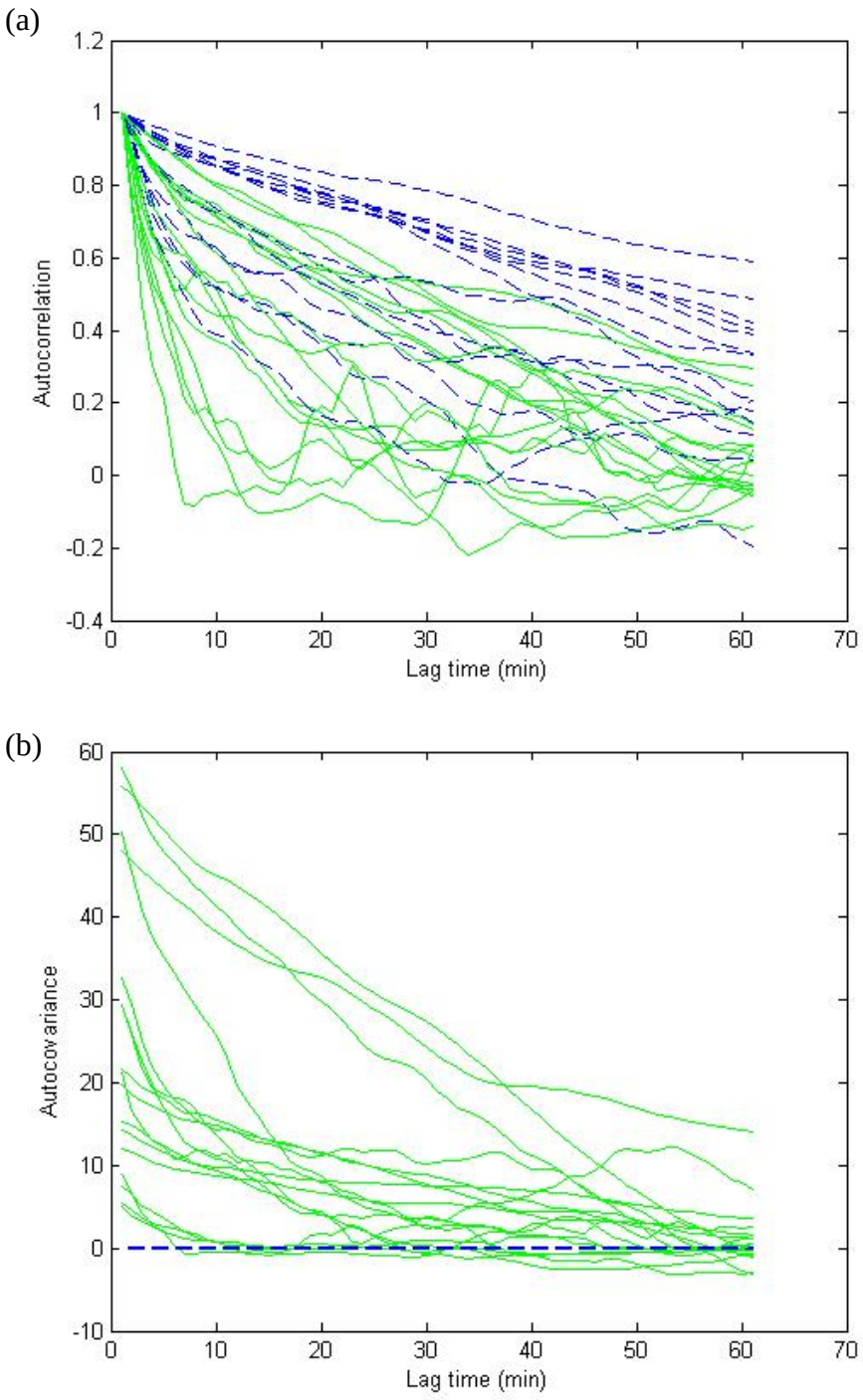

Figure 9. Correlograms for clearness index for August 2007 between 9 am PDT and 4 pm PDT at Las Vegas Springs Preserve: (a) autocorrelation coefficients and (b) autocovariances.

Note: One curve shown for each day in August 2007. Cloudy to partly cloudy days are shown in green solid lines; clear days shown with blue dashed lines.

(a)

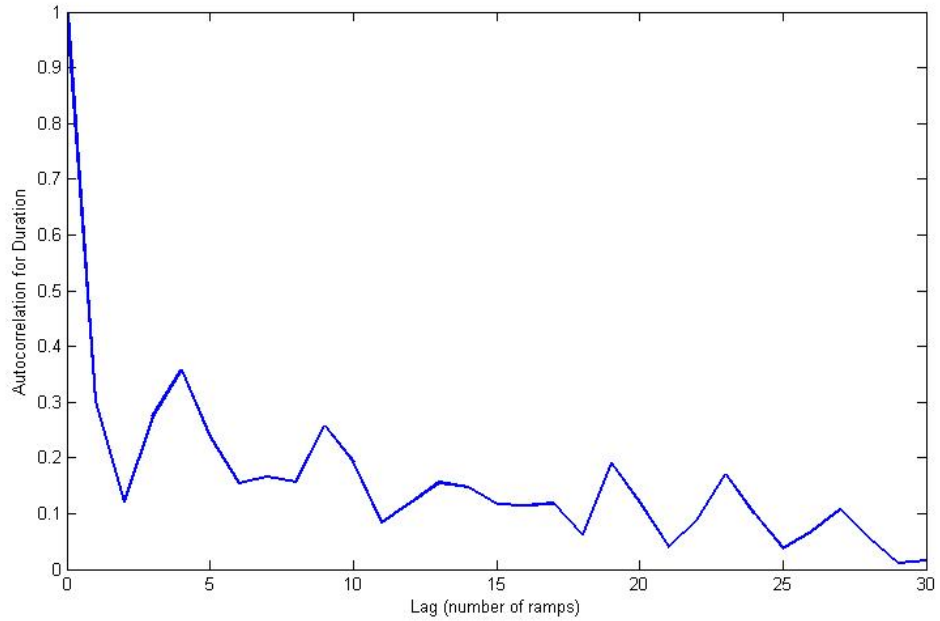
Autocorrelation for Duration
Lag (number of ramps)
0
0.1
0.2
0.3
0.4
0.5
0.6
0.7
0.8
0.9
1
0
5
10
15
20
25
30

(b)

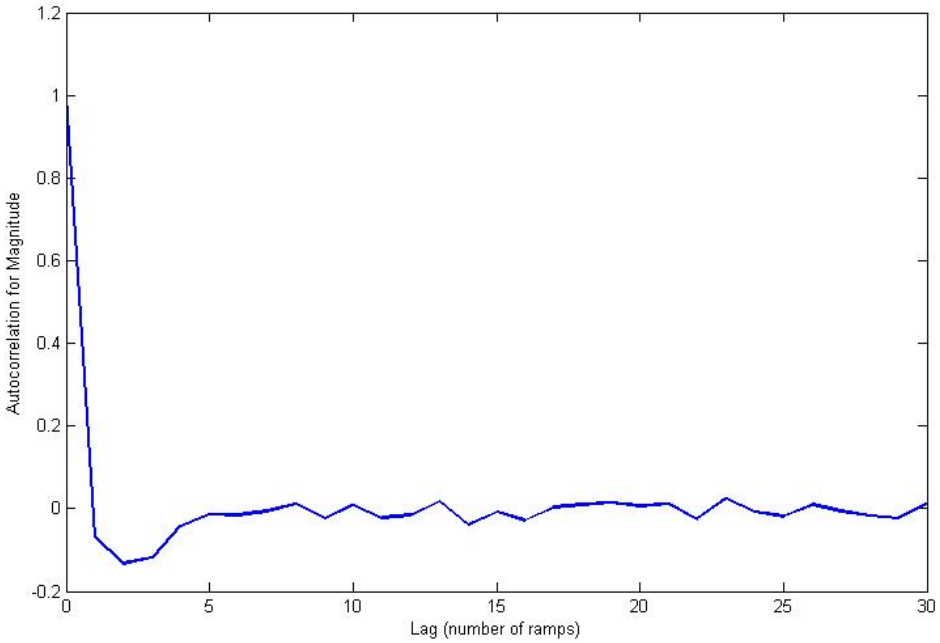
Autocorrelation for Magnitude
Lag (number of ramps)
-0.2
0
0.2
0.4
0.6
0.8
1
1.2
0
5
10
15
20
25
30

(c)

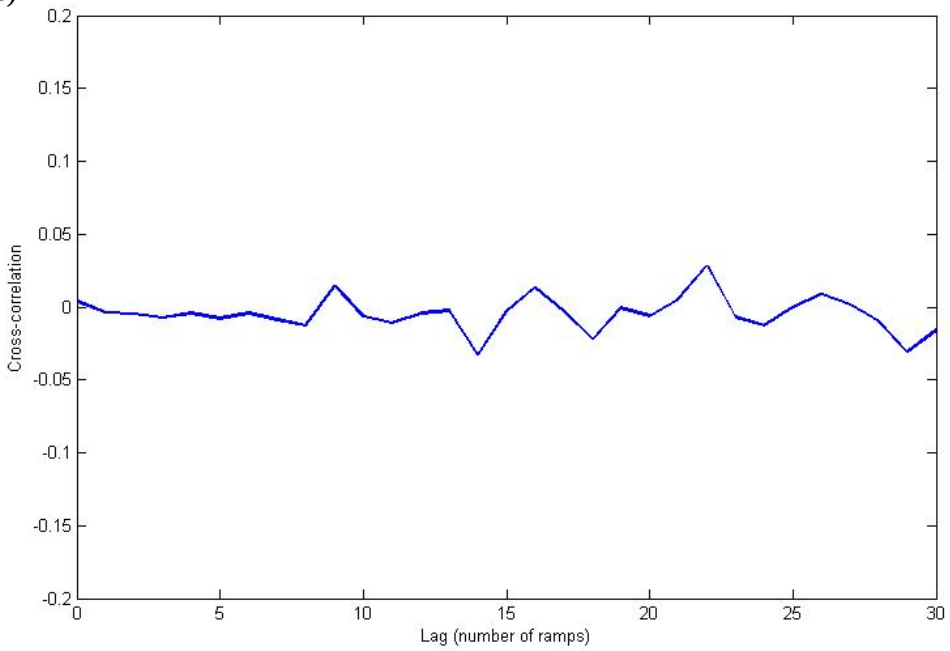

Figure 10. Correlograms for ramps in clearness index for August 2007 between 9 am PDT and 4 pm PDT, at Las Vegas Springs Preserve: (a) autocorrelation coefficient for ramp duration *T*; (b) autocorrelation coefficient for ramp magnitude *R*; and (c) cross correlation coefficient between ramp duration *T* and magnitude *R*.

3.2 Irradiance Data for Albuquerque

One-minute averages of irradiance were recorded by Sandia National Laboratories at its Photovoltaic Systems Evaluation Laboratory (lat. 35.05 N long. 105.54 W) for June 2010. Global horizontal irradiance was measured using a Kipp & Zonen CM2 pyranometer calibrated to a relative accuracy of +/- 3.5%. As was done for irradiance measurements for Las Vegas, the Atwater and Ball (1979 [22]) model for clear sky global irradiance is used to convert irradiance measurements to clearness index using the assumed model parameters listed in Table 1 to estimate a value for precipitable water for this period, with the result being 1.7 cm. Figure 11 shows recorded for Albuquerque, New Mexico, for June 1, 2009 to June 29, 2009 between 9am MDT and 4pm MDT.

Figure 11 shows that during this period most days exhibited variable irradiance levels, with only two days completely clear. These conditions contrast with conditions observed in August 2007 in Las Vegas, where 14 of 31 days were completely clear. The variable irradiance levels observed in Albuquerque are reflected in the clearness indices shown in Figure 12, and in histograms of irradiance levels and clearness index (Figure 13 and Figure 14, respectively) where the broad peaks representing cloudy conditions is larger than those for Las Vegas (Figure 4 and Figure 5, respectively).

The different proportions of clear and cloudy conditions between Las Vegas and Albuquerque are reflected in the histogram for ramps in irradiance (Figure 15). For Albuquerque the histogram shows fewer ramps of longer duration than observed for Las Vegas (Figure 8), resulting from the general persistence of variable irradiance conditions during June 2009 in Albuquerque. Comparison of histograms for ramps in clearness index and scatterplots of ramps (Figure 9 and Figure 16) yields similar observations.

Autocorrelations and autocovariance plots for duration and magnitude of ramps in clearness index for Albuquerque are similar to those for Las Vegas. Autocovariance (Figure 17b) is also effective at separating clear and cloudy days for Albuquerque, however, the presence of days that are mostly clear with brief periods of variable irradiance (e.g., June 21, 2009) result in autocovariance curves that are non-zero briefly (for short lags) but rapidly decay to zero. Autocorrelation curves for ramp duration and magnitude, and cross correlation between duration and magnitude (Figure 18) for clearness index in Albuquerque are similar to those for Las Vegas (Figure 10). Because irradiance levels were more variable in Albuquerque than in Las Vegas, more short duration ramps are present in the Albuquerque data which result in a more smoothly decaying autocorrelation plot for ramp duration (Figure 18a).

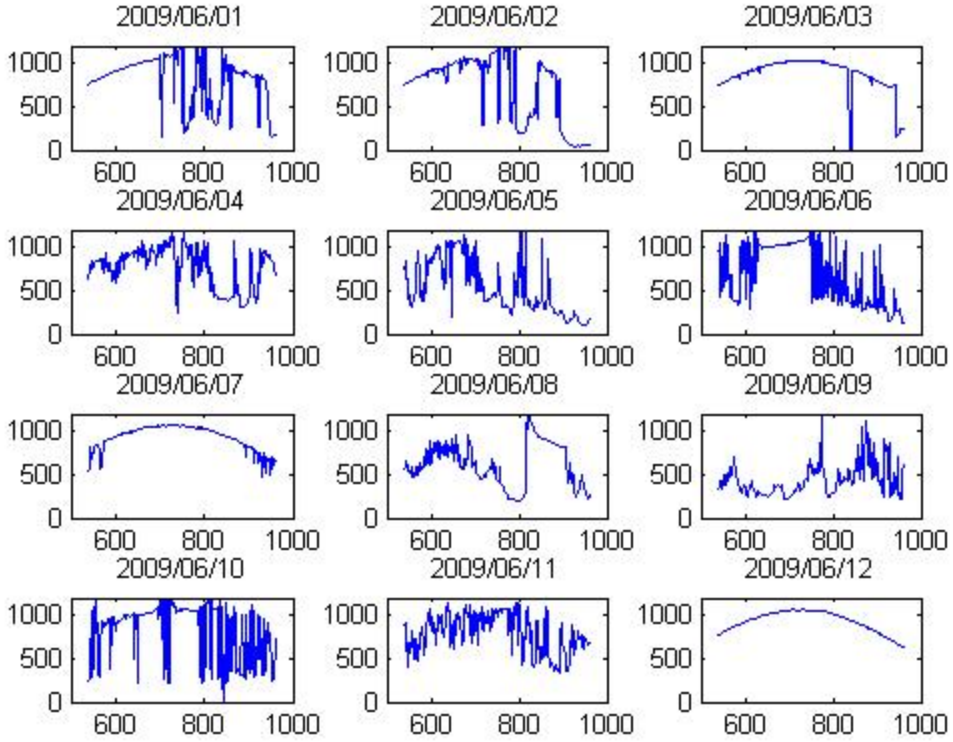
2009/06/01
2009/06/02
2009/06/03
2009/06/04
2009/06/05
2009/06/06
2009/06/07
2009/06/08
2009/06/09
2009/06/10
2009/06/11
2009/06/12
1000
500
0
600
800
1000

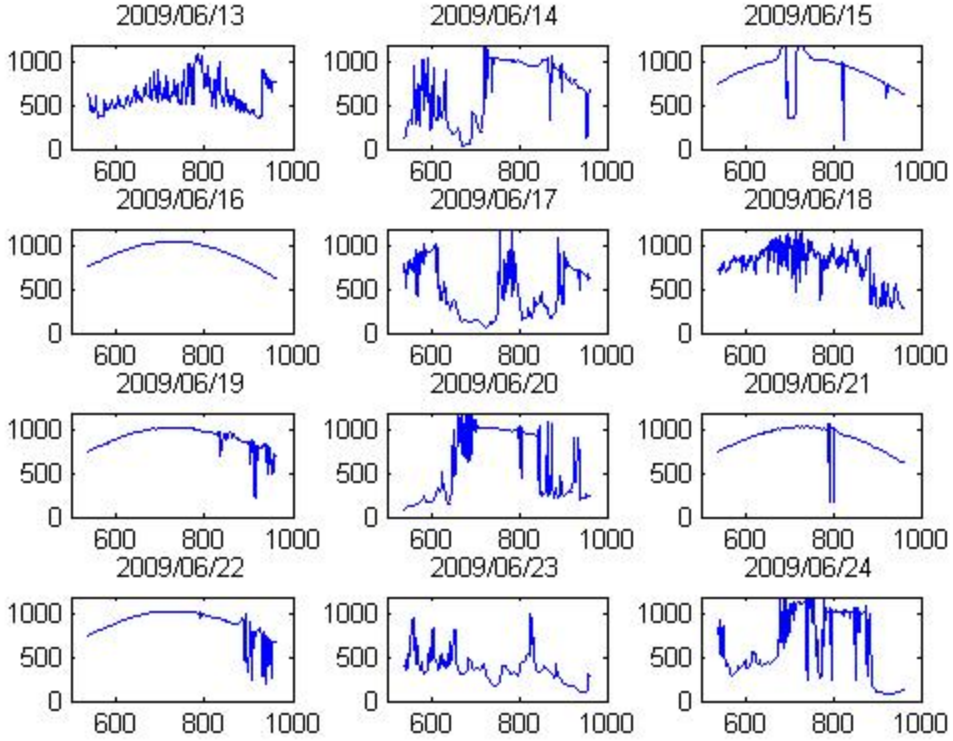
2009/06/13
2009/06/14
2009/06/15
2009/06/16
2009/06/17
2009/06/18
2009/06/19
2009/06/20
2009/06/21
2009/06/22
2009/06/23
2009/06/24
1000
500
0
600
800
1000

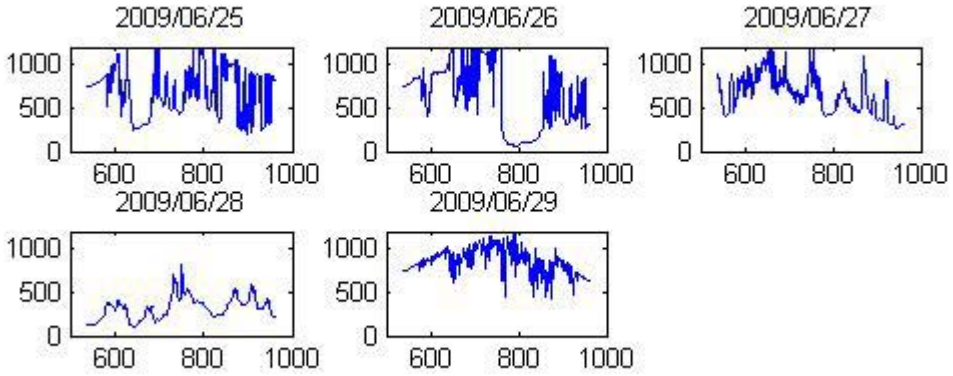

Figure 11. Irradiance recorded during June 2009 at Albuquerque, New Mexico between 9am MDT and 4pm MDT.

Note: *x*-axis units are minutes since midnight; *y*-axis is irradiance (W/m^2).

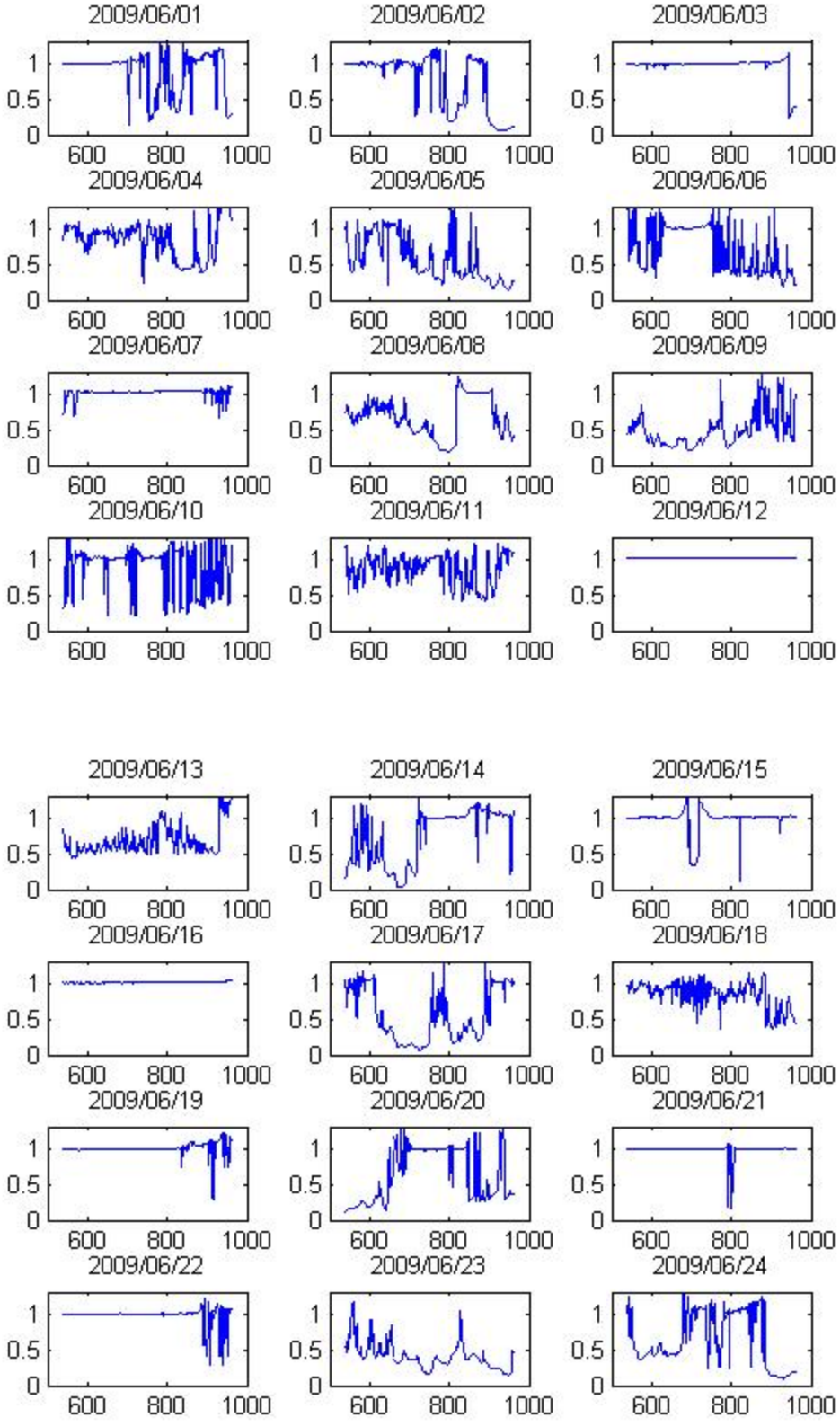
2009/06/01
2009/06/02
2009/06/03
2009/06/04
2009/06/05
2009/06/06
2009/06/07
2009/06/08
2009/06/09
2009/06/10
2009/06/11
2009/06/12
2009/06/13
2009/06/14
2009/06/15
2009/06/16
2009/06/17
2009/06/18
2009/06/19
2009/06/20
2009/06/21
2009/06/22
2009/06/23
2009/06/24
0
0.5
1
600
800
1000

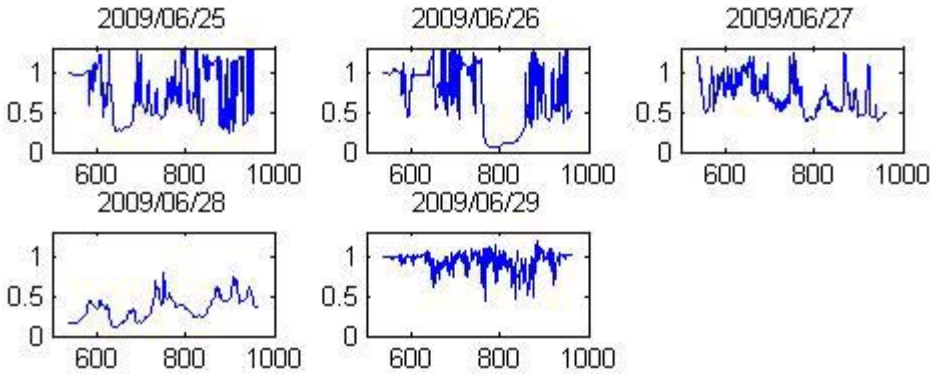

Figure 12. Clearness index for June 2009 at Albuquerque, New Mexico between 9am MDT and 4 pm MDT.

Note: *x*-axis units are minutes since midnight; *y*-axis is irradiance (W/m^2).

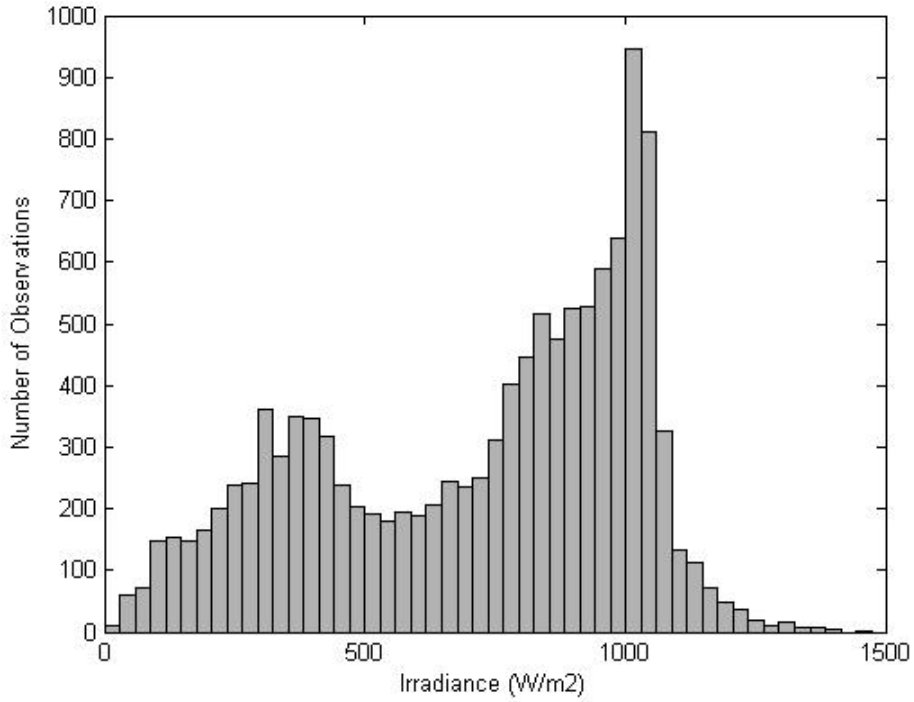

Figure 13. Frequency distribution of irradiance for June 2009, between 9 am MDT and 4 pm MDT, at Albuquerque, New Mexico.

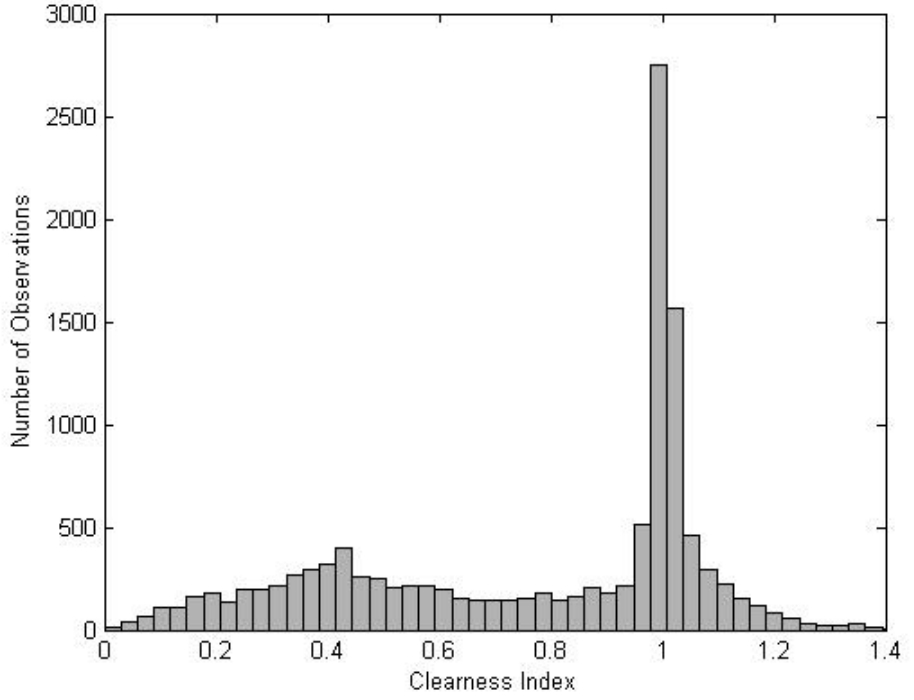

Figure 14. Frequency distribution of clearness index for June 2009, between 9 am MDT and 4 pm MDT, at Albuquerque, New Mexico.

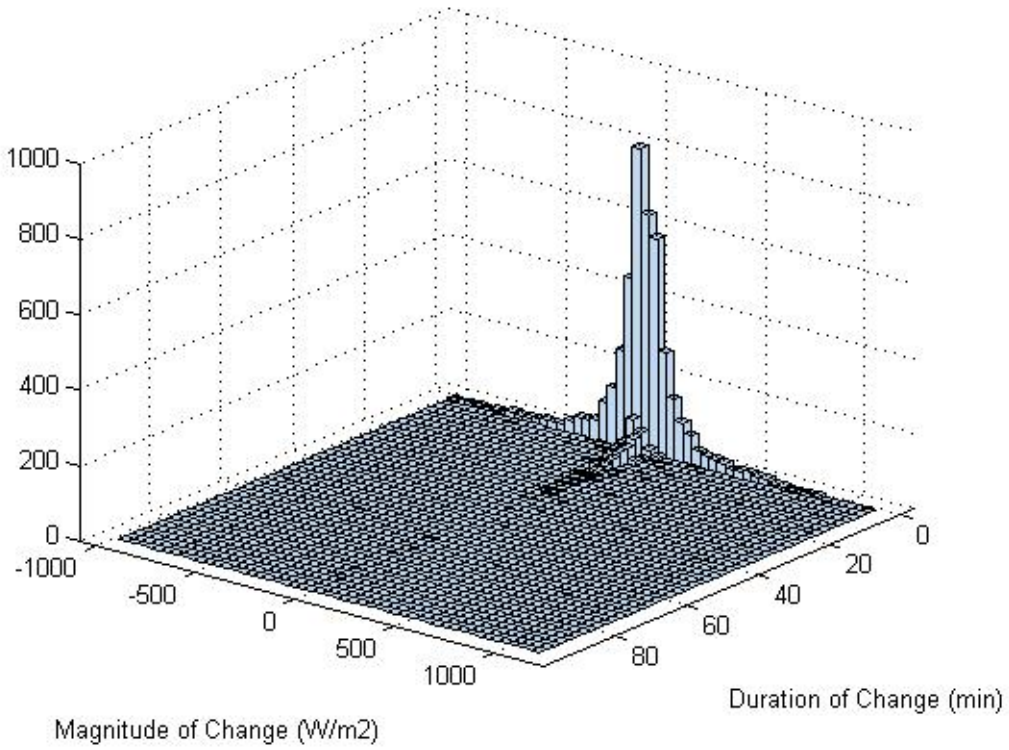

Figure 15. Bivariate histogram of ramps in irradiance calculated using piecewise linear approximation to irradiance for June 2009 between 9 am MDT and 4 pm MDT, at Albuquerque, New Mexico.

Note: Ramps calculated using piecewise linear approximation to irradiance.

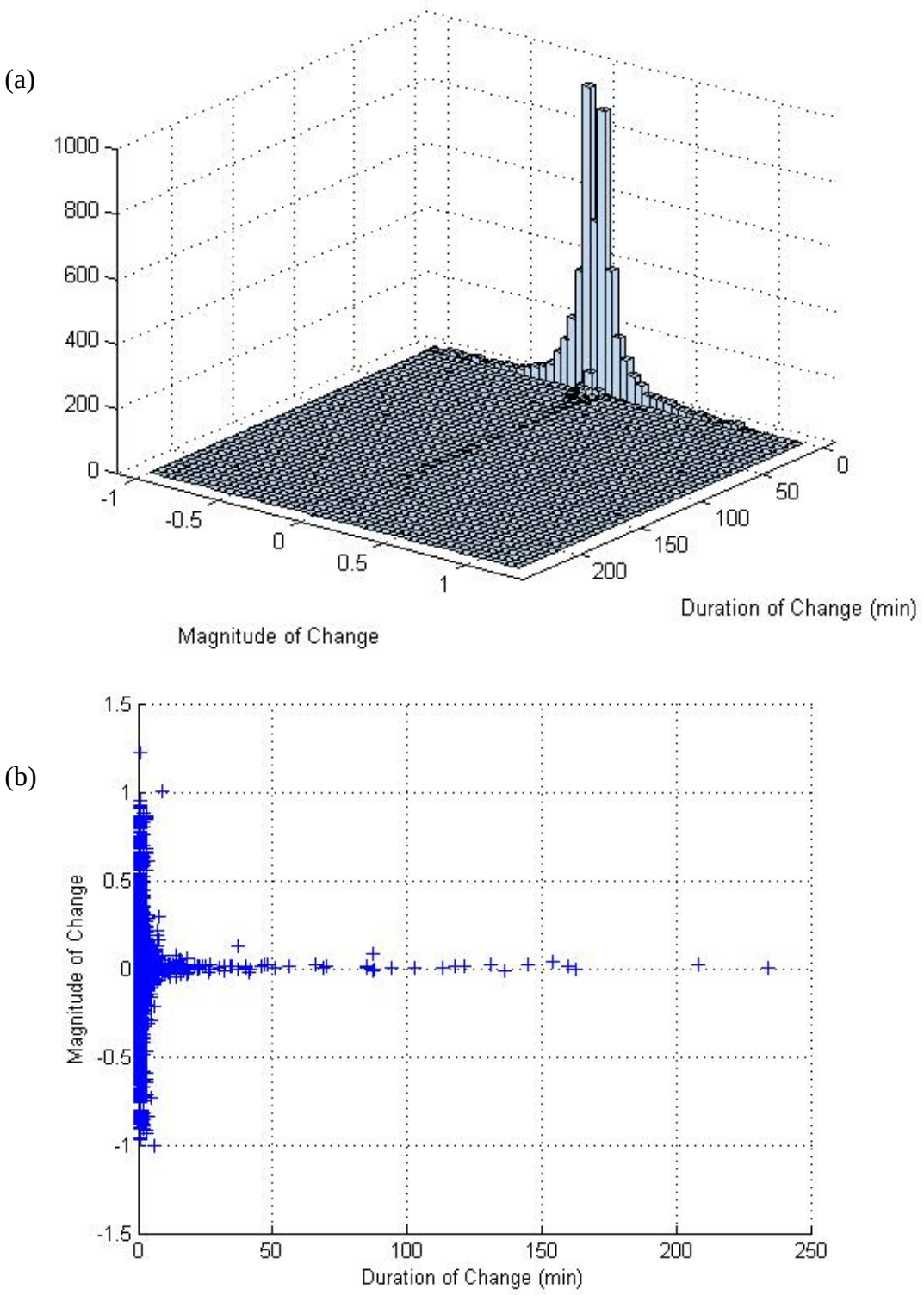

Figure 16. (a) Bivariate histogram of ramps in clearness index and (b) scatterplot of ramp duration and magnitude.

Note: Ramps calculated using piecewise linear approximation to irradiance for June 2009 between 9 am MDT and 4 pm MDT, at Albuquerque, New Mexico.

(a)

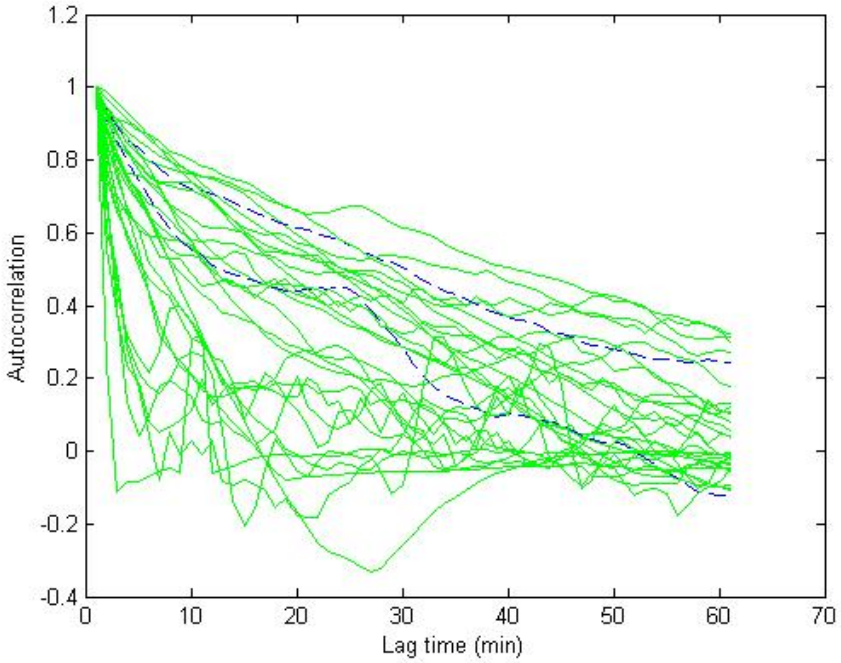

(b)

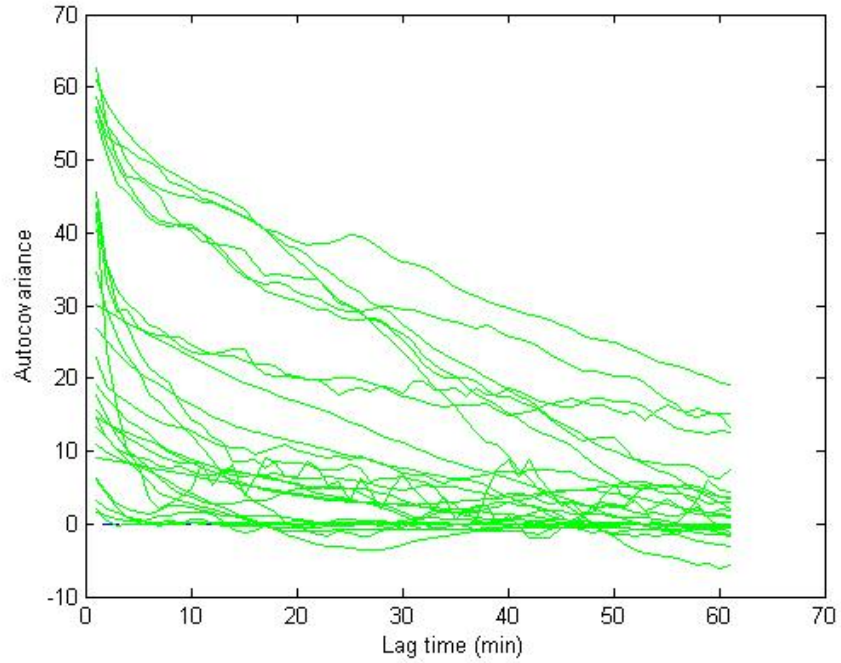

Figure 17. Correlograms for clearness index for June 2009 between 9 am MDT and 4 pm MDT at Albuquerque, New Mexico: (a) autocorrelation coefficients and (b) autocovariances.

Note: One curve shown for each day between June 1 and June 29, 2009. Cloudy to partly cloudy days are shown in green solid lines; clear days shown with blue dashed lines.

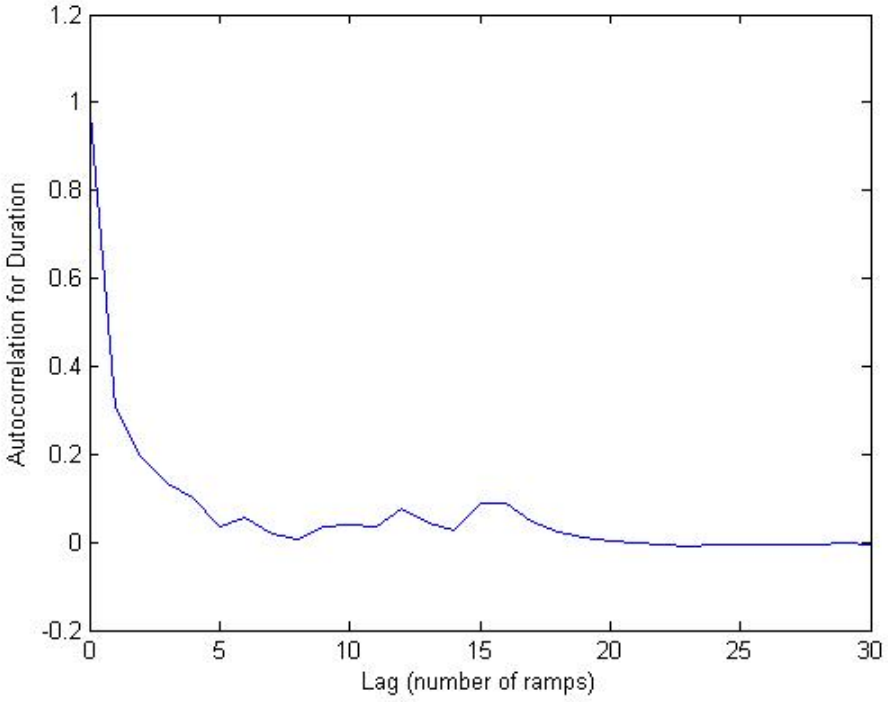
Autocorrelation for Duration
Lag (number of ramps)
1.2
1
0.8
0.6
0.4
0.2
0
-0.2
0
5
10
15
20
25
30

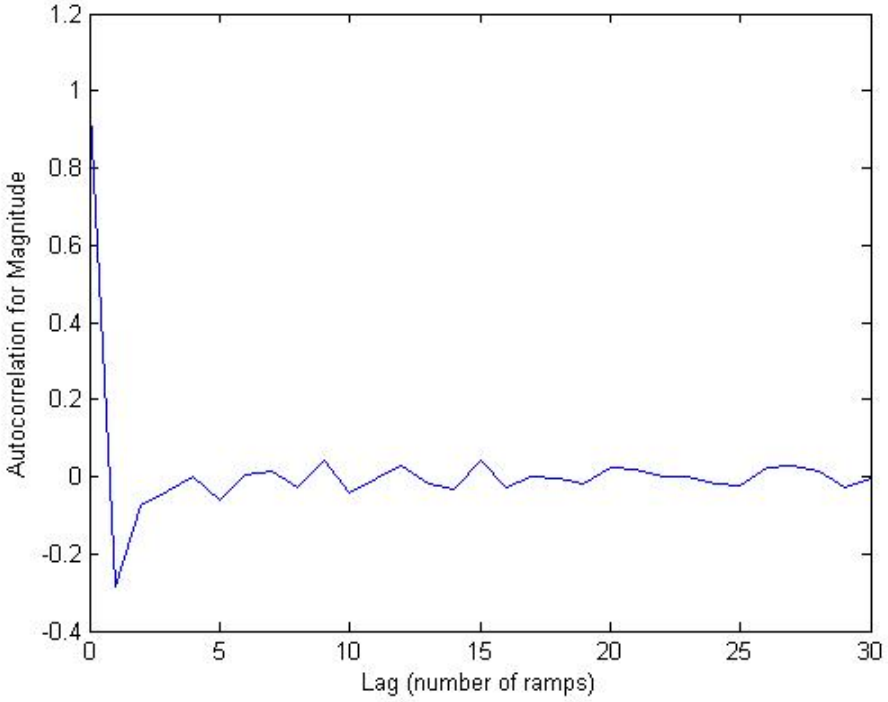
Autocorrelation for Magnitude
Lag (number of ramps)
1.2
1
0.8
0.6
0.4
0.2
0
-0.2
-0.4
0
5
10
15
20
25
30

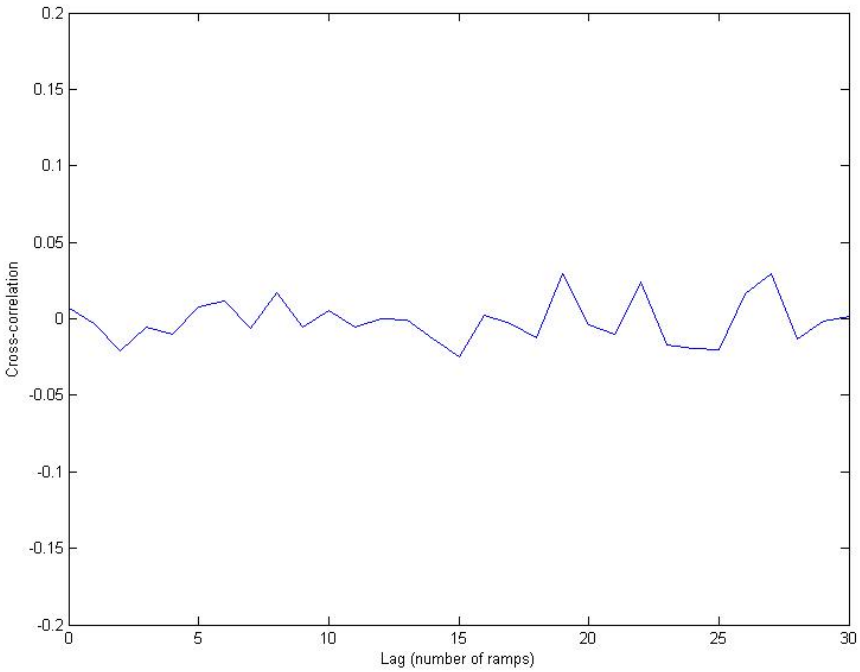

Figure 18. Correlograms for ramps in clearness index for June 2009 between 9 am MDT and 4 pm MDT, at Albuquerque, New Mexico: (a) autocorrelation coefficient for ramp duration *T*; (b) autocorrelation coefficient for ramp magnitude *R*; and (c) cross correlation coefficient between ramp duration *T* and magnitude *R*.

4. EVALUATION

In this report we propose three statistics that can be used to compare simulations of irradiance to observed data:

1. The frequency distribution of irradiance (or clearness index).

2. The bivariate distribution of ramps in irradiance (or clearness index).

3. The autocovariance and autocorrelation in the time series of clearness index.

In Section 3, we illustrate these statistics using irradiance data for Las Vegas, NV in August 2007 and for Albuquerque, NM in June 2009. Here we consider the extent to which these statistics characterize time series in irradiance and implications from these statistics for models that simulate irradiance.

4.1. Assessment of Statistics for Characterizing Time Series

The frequency distribution of irradiance is the basic statistic that characterizes a time series of irradiance. The distribution contains summary measures of irradiance such as the time series' mean and variance. Frequency distributions show the relative frequency at which different levels of irradiance are observed; time series with significantly different frequency distributions will result in different distributions of estimated power from a PV plant. Use of frequency distributions for both irradiance and for clearness index is likely redundant, because clear sky radiation models are deterministic and the available models have been shown to agree within a tight confidence interval (e.g., [23]; [28]) and hence one distribution may be obtained from the other.

Where changes in irradiance are of interest, the bivariate distribution of ramps in irradiance is important to consider in conjunction with the frequency distribution in irradiance. Time series with different bivariate distributions in ramps in irradiance exhibit changes in irradiance of different duration and/or magnitude, or exhibit different frequencies of occurrence of such changes. However, because the bivariate distribution of ramps does not contain information about the absolute irradiance level when the change began, it is possible to realize similar bivariate distributions for dissimilar time series. For example, a clear day would exhibit a bivariate distribution comprising many relatively short changes resulting from approximation of the diurnal irradiance levels with connected line segments. It is possible that a similar distribution of ramps would result during an overcast day, during which irradiance is much lower generally but changes in irradiance occur with similar durations and magnitudes as those that occur during a clear day.

Similarly, by itself the bivariate distribution of ramps in clearness index is insufficient to characterize changes in time series of irradiance. Because clearness index results from normalizing irradiance to clear sky conditions, a ramp in clearness index is essentially a fractional change in irradiance and is not informative about the magnitude of the absolute value of the change. Bivariate distributions in clearness index ramps are not interchangeable with bivariate distributions in irradiance ramps due to the absence of information regarding the magnitude of irradiance when the ramp began. However, bivariate distributions in clearness

index ramps are more suited to representing irradiance during clear days than are bivariate distributions of irradiance ramps. In the bivariate distribution of clearness index ramps, a clear day is indicated by a long duration ramp of little or no magnitude. In contrast, a clear day is represented in the bivariate distribution of irradiance ramps by a small number of ramps of moderate duration and magnitude; similar ramps may result from gradually changing cloud conditions during a cloudy day. We conclude that both bivariate distributions contain information that is informative about changes in irradiance and that both distributions should be considered.

When the time-ordering of irradiance levels is of interest, autocovariances and autocorrelation coefficients provide related but different information about the correlation between successive values of irradiance and clearness index. Autocorrelations for clearness index alone may not distinguish between time series with significantly different characteristics. For example, as demonstrated by Figure 9, autocorrelations do not distinguish between clear and cloudy conditions because these statistics are normalized by the variance in the time series. Autocorrelations during clear sky conditions may appear similar to those during cloudy conditions because variability is present during clear sky conditions, although of small magnitude. In contrast, autocovariances readily distinguish between clear and cloudy conditions. However, a wide range of autocovariance curves may be observed when partly to mostly cloudy conditions are present. Autocovariance and autocorrelation for time series of duration and magnitude of ramps in clearness index show that after a relatively few ramps neither duration nor magnitude is correlated. Moreover, because of the absence of ramps of both long duration and significant magnitude, there is essentially no cross-correlation between duration and magnitude in ramps.

As shown in Section 3.2, similar conclusions hold for irradiance observed in Albuquerque, NM, for a period with more variable irradiance than was observed in Las Vegas. The more variable irradiance levels observed in Albuquerque are reflected by corresponding shifts in the distributions of irradiance levels and clearness index as well as in the histograms of ramps in irradiance. Despite the increased variability, autocorrelations and autocovariance plots appear similar.

4.2. Implications for Simulating Irradiance

In concept a model for simulating irradiance would generate an ensemble of time series using an appropriate sampling or Monte Carlo method. For the results examined in Section 3, simply sampling a sequence of irradiance values from the frequency distribution for irradiance would not produce statistically consistent time series because this simple approach would be unlikely to produce distributions of ramps similar to those observed, nor would this approach preserve correlations between successive irradiance values. An autoregressive model for irradiance could be constructed from an autocorrelation curve, but this approach seems problematic due to the variation between curves and the inability to distinguish between clear and cloudy days using the autocorrelation curves. Moreover, the relatively slow decay of some of the autocorrelation curves may lead to autoregressive models of relatively high order.

Similarly, randomly sampling a sequence of ramps from the histograms shown in Figure 6 or Figure 8 is not likely to produce sequences of irradiance with successive clear days, as are observed in Figure 2. The predominance of short, small ramps in the distribution of ramps would preclude successive long ramps corresponding to clear days.

The major challenge apparent in simulating from the data presented in Section 3 is that irradiance and changes in irradiance have been pooled across time periods with significantly different behavior, namely, clear and cloudy days. Accordingly, a model for simulating irradiance is likely to require first separating periods into at least two categories, clear and not clear, and possibly further subdividing the category of not clear periods. An appropriate model would need to be constructed to generate the sequence of clear and not clear periods. Then, conditional on a period being clear or not clear, it may be possible to use the statistics presented above to formulate an appropriate model to simulate irradiance during that period. This nested approach may overcome the difficulties indicated above for approaches that randomly sample from the distributions for irradiance and/or ramps in irradiance.

SUMMARY

Three statistics for characterizing time series of irradiance have been presented that together allow time series of simulated irradiance to be compared to measured data for model validation:

1. The frequency distribution of irradiance (or clearness index).

2. The bivariate distribution of ramps in irradiance (or clearness index).

3. The autocovariance and autocorrelation in the time series of clearness index.

How these statistics are applied and interpreted depends on the intent of the simulation or study. If the purpose is to evaluate the uncertainty in the long term annual energy production from a PV system, it is likely that only the frequency distribution of the irradiance is important to characterize. However, if a study is interested in strategies for managing ramps in power generation, evaluating energy management options such as battery storage systems, or designing demand-side load management schemes, the magnitude and duration of ramps and possibly their autocovariance and autocorrelation characteristics may be important to simulate accurately.

The three statistics have been computed for one month (August 2007) of one-minute irradiance averages measured in Las Vegas, NV and for one-minute irradiance averages measured in Albuquerque, NM, in June 2009. Plots of irradiance and clearness index demonstrate that clear-sky conditions were observed less often in Albuquerque than in Las Vegas, and consequently irradiance levels were more variable in Albuquerque. The different levels of irradiance variability are readily apparent in the frequency distributions for irradiance and clearness index. However, the effects of different levels of irradiance variability are less apparent in the bivariate distributions of ramps and in plots of autocovariance and autocorrelation coefficients. Future work should investigate the degree to which these statistics are sensitive irradiance variability for a wide range of conditions. In addition, the effect on these statistics of different tolerances for the piecewise linear fitting algorithm should be evaluated.

Results of this analysis suggest that periods of clear sky conditions should be separated from partly cloudy periods and separate models formulated to simulate conditions during each period, as statistics obtained without segregating clear and non-clear periods appear to be difficult to reproduce with simulation models.

The three statistics presented here are based on traditional approaches to characterizing data and time series. Other approaches, such as wavelet decomposition (e.g., [7]; [8]) may prove valuable for developing simulation approaches for irradiance. These and other approaches will be investigated in subsequent efforts.

8. REFERENCES

1. GE Energy, (2010). Western Wind and Solar Integration Study, National Renewable Energy Laboratory.

2. Marion, W. and K. Urban (1995). User's Manual for TMY2s Typical Meteorological Years, National Renewable Energy Laboratory.

3. Wilcox, S. and W. Marion (2008). Users Manual for TMY3 Data Sets, National Renewable Energy Laboratory.

4. King, D.L., W. E. Boyson, J. A. Kratochvill (2004). Photovoltaic Array Performance Model, Sandia National Laboratories, SAND2004-3535.

5. Sun, Y.-C. and R. Kok (2007). "A solar radiation model with a Fourier transform approach." Canadian Biosystems Engineering **49**: 7.17 - 7.24.

6. Baldasano, J. M., J. Clar, et al. (1988). "Fourier Analysis of Daily Solar Radiation Data in Spain." Solar Energy **41**(4): 327-333.

7. Woyte, A., R. Belmans, et al. (2007). "Localized Spectral Analysis of Fluctuating Power Generation from Solar Energy Systems." EURASIP Journal on Advances in Signal Processing **2007**: 1-8.

8. Woyte, A., R. Belmans, et al. (2007). "Fluctuations in instantaneous clearness index: Analysis and statistics." Solar Energy **81**: 195-206.

9. Tovar-Pescador, J. (2008). Modelling the Statistical Properties of Solar Radiation and Proposal of a Technique Based on Boltzmann Statistics. Modeling Solar Radiation at the Earth's Surface: Recent Advances. V. Badescu. Berlin, Springer-Verlag**:** 55-91.

10. Glasbey, C. A. (2001). "Nonlinear autoregressive time series with multivariate Gaussian mixtures as marginal distributions." Applied Statistics **50**: 143-154.

11. Kuszamaul, S., A. Ellis, et al. (2010). Lanai High-Density Irradiance Sensor Network for Characterizing Solar Resource Variability of MW-Scale PV System. 35th IEEE PVSC, Honolulu, HI.

12. Gansler, R. A., S. A. Klein, et al. (1995). "Investigation of minute solar radiation data." Solar Energy **55**(1): 21-27.

13. Tovar, J., F. J. Olmo, et al. (1998). "One-minute global Irradiance probability density distributions conditioned to the optical air mass." Solar Energy **62**(6): 387-393.

14. Tovar, J., F. J. Olmo, et al. (1999). "One-minute kb and kd probability density distributions conditioned to the optical air mass." Solar Energy **65**(5): 297-304.

15. Tovar, J., F. J. Olmo, et al. (2001). "Dependence of one-minute global irradiance probability density distributions on hourly irradiation." Energy **26**: 659-668.

16. Bristol, E. H. (1990). Swinging Door Trending: Adaptive Trend Recording? ISA National Conference Proceedings.

17. Makarov, Y. V., C. Loutan, et al. (2009). "Operational Impacts of Wind Generation on California Power Systems." IEEE Transactions on Power Systems **24**(2): 1039-1050.

18. Horst, J. A. and I. Beichl (1996). Efficient piecewise linear approximation of space curves using chord and arc length. Proceedings of the SME Applied Machine Vision '96 Conference.

19. Tomson, T., V. Russak, A. Kallis (2008). Dynamic Behavior of Solar Radiation. Modeling Solar Radiation at the Earth's Surface: Recent Advances. V. Badescu. Berlin, Springer-Verlag: 257-281.

20. Skartveit, A. and J. A. Olseth (1992). "The probability density and autocorrelation of short-term global and beam irradiance." Solar Energy **49**(6): 477-487.

21. Walkenhorst, O., J. Luther, et al. (2002). "Dynamic annual daylight simulations based on one-hour and one minute means of irradiance data." Solar Energy **72**(5): 385-395.

22. Atwater, M. A. and J. T. Ball (1978). "A numerical solar radiation model based on standard meteorological observations." Solar Energy **21**: 163-178.

23. Bird, R. E. and R. L. Hulstrom (1981). A Simplified Clear Sky Model for Direct and Diffuse Insolation on Horizontal Surfaces, Solar Energy Research Institute.

24. Flowers, E. C., R. A. McCormick, et al. (1969). "Atmospheric Turbidity over the United States, 1961-1966." Journal of Applied Meteorology **8**: 955-962.

25. Suehrcke, H. and P. G. McCormick (1988). "The frequency distribution of instantaneous insolation values." Solar Energy **40**(5): 413-422.

26. Emck, P. and M. Richter (2008). "An Upper Threshold of Enhanced Global Shortwave Irradiance in the Troposphere Derived from Field Measurements in Tropical Mountains." Journal of Applied Meteorology and Climatology **47**: 2828-2845.

27. Shimazaki, H. and S. Shinomoto (2007). "A Method for Selecting the Bin Size of a Time Histogram." Neural Computation **19**: 1503-1527.

28. Ineichen, P. (2006). "Comparison of eight clear sky broadband models against 16 independent data banks." Solar Energy **80**: 468-478.

DISTRIBUTION

All Electronic Copies

U.S. Department of Energy

1	K. Lynn	kevin.lynn@hq.doe.gov
1	M. Kliggett	michael.cliggett@ee.doe.gov

National Renewable Energy Laboratory

1	D. Renne	David.Renne@nrel.gov
1	B. Kroposki	Benjamin.Kroposki@nrel.gov
1	K. Orwig	Kirsten.Orwig@nrel.gov
1	T. Stoffel	Thomas.Stoffel@nrel.gov
1	R. George	Ray.George@nrel.gov
1	D. Myers	Daryl.Myers@nrel.gov
1	M. Sengupta	Manajit.Sengupta@nrel.gov
1	M. Hummon	Marissa.Hummon@nrel.gov

Other Recipients

1	A. Mills	admills@lbl.gov
1	R. Guttromson	ross.guttromson@pnl.gov
1	J. Kleissl	jkleissl@ucsd.edu
1	A. Cronin	cronin@physics.arizona.edu
1	F. Vignola	fev@uoregon.edu
1.	C. Lenox	Carl.Lenox@sunpowercorp.com
1	L. Nelson	lauren.nelson@sunpowercorp.com
1	T. Key	tkey@epri.com
1	T. Hoff	tomhoff@cleanpower.com
1	V. Chadliev	VChadliev@nvenergy.com
1	R. Flood	ronald.flood@aps.com
1	C. Gueymard	Chris@SolarConsultingServices.com
1	A. Kankiewitcz	kankie@WindLogics.com
1	J. Blatchford	jblatchford@caiso.com
1.	G. Stevens	GStevens@NavigantConsulting.com

Sandia National Laboratories

1	0735	G. T. Klise,	6733	
1	1033	J. S. Stein,	6352	
1	1033	C. W. Hansen,		6352
1	1033	J. S. Stein,	6335	
1	0406	R. N. Chapman,		5713
1	0613	R. G. Jungst,	2548	

1	0614	T. D. Hund,	2547
1	0614	D. Ingersoll,	2546
1	0734	W. I. Bower,	6364
1	0734	V. P. Gupta,	6364
1	0734	J. S. Nelson,	6338
1	0734	E. B. Stechel,	6383
1	0781	R. E. Fate,	6473
1	0982	M. Brown,	5737
1	1033	C. J. Hanley,	6352
1	1033	C. P. Cameron,	6352
1	1033	W. Boyson	6352
1	1033	D. Riley,	6352
1	1033	M. A. Quintana,	6352
1	1033	J. E. Granata,	6352
1	1033	S. Gonzalez,	6352
1	1033	A. Ellis,	6352
1	1033	S. S. Kuszmaul,	6352
1	1033	B.L. Schenkman,	6353
1	1108	J. J. Torres,	6351
1	1108	J. D. Boyes,	6353
1	1127	J. R. Tillerson,	6363
1	1127	C.K. Ho,	6363
1	1127	T. R. Mancini,	6363
1	1127	G. J. Kolb,	6363
1	1137	E. H. Richards,	6733
1	0899	Technical Library	9536


Sandia National Laboratories